Shear strength of reinforced mortar beams containing polyvinyl alcohol fibre (PVA)

RESEARCH PAPER

Shear Strength of Reinforced Mortar Beams Containing Polyvinyl Alcohol Fibre (PVA)

Mohamed Said[1] · Wael Montaser[2] · Ahmed S. Elgammal[2] · Amr H. Zahir[3] · Ibrahim G. Shaaban[4]

Abstract

The current study aims to assess the shear behaviour of reinforced mortar beams including Polyvinyl Alcohol Fibre (PVA) ranges from 0 to 2.25%, fly ash (55%) and silica fume (15%). Fourteen beams were experimentally tested under two concentrated loads. In addition, a finite element model was developed to predict the crack pattern, load–deflection, energy absorption, and shear strength results of the test beams. The studied variables were different percentages of PVA fibres, shear span to depth ratio (*a/d*), and transverse reinforcement (stirrups) ratio. The fly ash and silica fume were kept constant in all the studied mixes to achieve a compressive strength above 55 MPa at the time of testing (90 days) and to improve PVA-mortar properties. It was found that the inclusion of PVA improves the shear behavior of the tested beams in terms of crack pattern and ductility. It was observed also that reducing *a/d* led to enhancing the shear capacity without changing the mode of failure. In addition, PVA played the same role as the stirrups and their effect on the ultimate shear capacity was increased with reducing the volume of stirrups. Moreover, the PVA fibres were more effective in lower shear span to depth ratio (*a/d* = 1.5) giving an enhancement of shear resistance of 221%. The non-linear finite element model showed excellent agreement with the experimental results and the ratio of the predicted to experimental ultimate strength ranged between 0.91 and 1.09. The authors recommend a combination of fly ash, silica fume and at least 1.5% PVA in the presence of minimum stirrups reinforcement (5Φ6/m) or adding 2.25% PVA without stirrups to achieve adequate shear behaviour and to improve the ductility of PVA-mortar beams.

Keywords PVA · Mortar · Shear of beams · Fly ash · Silica fume · Non-linear finite element modeling

✉ Ibrahim G. Shaaban
ibrahim.shaaban@uwl.ac.uk

Mohamed Said
mohamed.abdelghaffar@feng.bu.edu.eg

Wael Montaser
wmontaser.eng@o6u.edu.eg

Ahmed S. Elgammal
eng.a.sherif93@gmail.com

Amr H. Zahir
amr_h_zaher@yahoo.com

[1] Civil Engineering Department, Faculty of Engineering (Shoubra), Benha University, Banha, Egypt

[2] Construction and Building Department, Faculty of Engineering, October 6 University, Al Mehwar Al Markazi, Egypt

[3] Structural Engineering Department, Faculty of Engineering, Ain Shams University, Cairo, Egypt

[4] School of Computing and Engineering, University of West London, London, UK

1 Introduction

Polyvinyl Alcohol fibre (PVA) is an environment friendly fibre with excellent alkali resistance. PVA fibre is economic, exhibits higher tensile strength and elastic modulus compared to polypropylene (PP) fibre [1]. Researchers [1–4] reported that the overall cost of mortar/concrete composites including PVA, such as Engineered Cementitious Composites (ECC), can be reduced by using an optimized dosage of micro-fibres and local materials including cement, fine aggregate, cement replacement materials such as fly ash and silica fume, and chemical admixtures. Iqbal Khan et al. [4] reported that the use of coarse aggregates increased the fibre balling, which reduced the micro-fibre dispersion effectiveness. Therefore, researchers [5, 6] eliminated the coarse aggregates in their mixes and only smaller amount of fine sand was used to control fracture toughness of matrix for PVA-mortar

composite production. Zhu et al. [7] reported the benefit of adding silica fume and fly ash in improving durability and compressive strength of PVA-mortar composite elements. Kanda et al. [8], used PVA fibres to produce ECC and they reported that the PVA is the main contributor to achieve the high strain hardening and ductility for ECC. Furthermore, Kanda et al. [9] described the design concept and material characteristics of PVA composite mortar elements. They showed that composites containing PVA exhibited a remarkably ductile tensile property with more than 1% tensile strain capacity, which in turn, has enhanced structural performance in seismic conditions.

Alyousif et al. [10] studied the shear behaviour of PVA-mortar beams cast with fly ash and different shear span lengths. The test results showed that the behaviour of these beams under shear was, in most cases, much better than that of conventional reinforced concrete beams without PVA. The strength, stiffness, ductility and energy absorption capacity of mortar beams with PVA were found to be significantly higher than those of the corresponding reinforced concrete beams without PVA, to varying degrees, based on the shear span to depth ratio. Paegle et al. [11] also studied the shear behaviour of PVA-mortar beams. Their experimental program consisted of reinforced mortar beams with short (8 mm) randomly distributed PVA fibre and conventional reinforced concrete counterparts for comparison with varying shear reinforcement arrangements. The results demonstrated that the PVA-mortar beams had better shear resistance, better control of crack sizes, and a more ductile shear failure compared to the conventional reinforced concrete beams. Liu et al. [12] reported that adding high content of fly ash (67%) to PVA-mortar composites resulted in self-healing of micro-cracks in structural elements under sulfate and chloride attack.

Ismail et al. [13] studied the shear behaviour of large-scale composite beams reinforced with different types of PVA and steel fibres (PVA8, PVA12, PP19, and long steel fibres, SF13). Their beams showed better performance in terms of cracking behaviour, shear capacity, ductility and energy absorption compared with normal reinforced concrete beams. Beams reinforced with PVA-8 fibres showed the highest shear strength and ductility compared to the beams containing other polymeric fibres. Longer PVA fibres appeared to be less efficient than shorter ones. The beam reinforced with PP19 showed the lowest performance, while the use of SF13 proved to be the most effective in improving the first crack load, ultimate load, ductility and energy absorption capacity. The researchers reported that the fly ash range (50–65%) and silica fume (5–15%) were the best combination for improving mechanical properties and durability aspects of PVA-mortar/concrete elements. This improvement was optimum when testing was conducted at the age of 90 days [7, 14, 15], because the pozzolanic reaction of silica fume and fly ash takes place after the initial hydration of cement and continues to 90 days and beyond [12, 15].

In the above reviewed literature, the importance of PVA fibres in improving the ductility of composite mortar was reported. The negative effect of coarse aggregate on the efficiency of PVA fibres was addressed. The positive effect of PVA with fly ash on the shear behaviour of mortar beams was mentioned. The improvement of PVA-mortar composite elements durability by adding silica fume (5–15%) and fly ash (50–65%) with PVA fibres was also reported.

2 Research Significance

Based on the research gap from the above literature review, the current study aims to investigate the shear behaviour of PVA-reinforced mortar beams containing a fixed content of fly ash (55%) and silica fume (15%), as recommended in the literature, and different percentages of PVA up to 2.25%. The research focuses on the effect of PVA in the presence of silica fume and fly ash after curing for 90 days on the structural behaviour and shear strength of studied beams. This will be achieved by testing 17 mortar beams containing different percentages of PVA with and without stirrups. Finite element modeling of the test beams was carried out using ANSYS to predict the crack pattern, load–deflection, and shear capacity results.

3 Experimental Program

3.1 Constituent Materials

The mix ingredients used throughout this investigation were Portland cement, fly ash, silica fume, polyvinyl alcohol (PVA) micro-fibres, natural siliceous sand, water, high range water reducer (HRWR), and reinforcing steel. The properties of these materials are given in the following sections.

3.1.1 Cement and Cement Replacement Materials

A grade 52.5 Portland cement was supplied by a local Egyptian factory, and is compatible with European standards [16]. Type F fly ash was obtained from CEMENTRAC Company for Cement Exporting. Fly ash complied with ASTM C 618 [17]. The silica fume was supplied by Sika Egypt for Construction Chemicals and it was complied with ASTM C 1240 [18]. The physical and chemical properties of cement replacement materials are shown in Tables 1 and 2 (provided by the supplier). In addition, the

physical and chemical properties of cement is presented in Table 3.

3.1.2 Polyvinyl Alcohol Fibre (PVA)

Different volume percentages of polyvinyl alcohol (PVA) fibres (0.75, 1.5, and 2.25%) were used in the mortar beams. The properties of PVA fibre are listed in Table 4 (provided by the supplier). The same mechanical properties PVA fibres were presented by Cao [19] and Said et al. [20]

3.1.3 Sand

Fine aggregate, used in sample preparation, was natural siliceous sand. The fine aggregate was clean, free of impurities and with no organic compounds with fineness modulus 2.84. Sieve analysis test was carried out in accordance with the ESS No. 1109/2002 [21] and the test results are shown in Table 5. Moreover, the sieve analysis curve of the fine aggregate is presented in Fig. 1.

3.1.4 Water and High Range Water Reducer

Potable tap water is used for mixing and curing of the test specimens. Polycarboxylic High Range Water Reducer (HRWR) from BASF Construction Chemicals (Master Glenium RMC 315) complying with BS EN 934-2 [22] was used. The objective of adding HRWR was to ensure that the PVA fibres were well-dispersed in the mixes and to achieve workability as indicated by a slump of 60 mm ± 10 mm.

3.1.5 Reinforcing Steel

The longitudinal reinforcement for the beams was high tensile steel (40/60) having 450 MPa yield stress. Mild steel (24/35) having 240 MPa yield stress was used for stirrups. The size of bars used for longitudinal reinforcement was18 mm diameter and for the stirrups, it was 6 mm diameter. The steel reinforcement properties were according to [23, 24].

Table 1 Properties of the used silica fume

SiO_2	> 88.9%
Moisture	< 0.57%
Alkalis like Na_2O	< 0.5%
Free CaO	< 0.1%
Free SI	0.14%
Free Cl%	0.02%
SO_3	< 0.25%
L.O.I (incl. carbon)	< 4.5%
Specific surface	~ 20 m^2/g
Size	~ 0.15 microns

Table 2 Properties of the used fly ash

Density (Kg/m^3)	2150
Activity index % (after 28 days)	77.5
Activity index % (after 90 days)	85.6
Soundness (mm)	1
Fineness %	22.43
LOI %	3.82
SiO_2%	57.87
Al_2O_3%	26.12
Fe_2O_3%	5.68
CaO%	1.163
SO_3%	< 0.00010
Alkalis%	2.46
Free CaO	0.03
CI %	< 0.00020
Reactive SiO_2%	40.34
Blaine (cm^2/g)	3330

Table 3 Physical and mechanical properties of cement

Property	Measured value
Fineness (mm^2/N)	3260
Specific gravity	3.15
Soundness (expansion, %)	0.50
Initial setting time (min.)	75’
Final setting time (min.)	180’
Crushing strength (MPa)	
3 days	23.9
7 days	26.52
28 days	35
Silica dioxide (SiO_2) %	21.45%
Aluminum oxide (Al_2O_3) %	5.80%
Iron oxide (Fe_2O_3) %	3.60%
Calcium oxide (CaO) %	63.63%
Magnesium oxide (MaO) %	1.4%
Sulphur trioxide (SO_3) %	3.17%
Moisture %	–
Loss due to ignition %	4.10%

Table 4 Properties of the polyvinyl alcohol fibres (PVA)

Length (lf) (mm)	Shape	Diameter (ϕf) (mm)	Tensile strength (MPa)	Elastic modulus (GPa)	Density (ρ) (g/cm^3)	Elongation (%)
12	Monofilament	0.04	1620	42.80	1.3	7.0

3.2 Mixing Process, Specimen Preparation, and Curing

Trial mixes were carried out varying the percentage of water binder ratio (w/b) to obtain the required f_{cu} (> 55 MPa at 90 days). Finally, the (w/b) ratio and sand to binder ratio were kept constant for all mixes at 0.33 and 0.8, respectively. The fly ash content was 55% and silica fume content was 15% of the total binder (Portland cement + fly ash + silica fume) as recommended in literature. HRWR was added with dosage ranges from 0.9 to 1.25% by weight of binder. The final quantities required by weight for one cubic meter of fresh concrete for the specimens are given in Table 6. The mixing process was according to the method described by Zhou et al. [25] to achieve good fibre dispersion. At the final stage of mixing, all materials were mechanically mixed in a drum mixer for 2 min and cast in the wooden forms, in which the reinforcing steel cages were previously placed. The poured PVA-mortar was then vibrated with an electrical Poker vibrator and the final surface was smoothed using a trowel. The forms were removed after 24 h from casting and specimens were kept under wet burlap, sprayed with water twice a day for 28 days and then kept in laboratory atmosphere for 90 days until they were tested.

To test the mechanical properties of the PVA-mortar composite, companion samples from the same mixes were prepared during casting the beam specimens. These samples were de-moulded 24 h after casting and were continuously water cured for 28 days (except for the cube samples that were tested for compressive strength at 7 days). Thereafter, these samples were kept in the laboratory near their corresponding beam samples until their testing age (i.e. some cubes were tested for compressive strength at 28 and 56 days, whilst the remainder of the samples were tested at 90 days).

Table 5 Sieve analysis test results for fine aggregates

Sieve size (mm)	Retained on each size (gm.)	Cumulative retained	Cumulative retained %	Passing %
40	0	0	0	100
20	0	0	0	100
10	0	0	0	100
5	5	5	0.5	99.5
2.5	32	37	3.7	96.3
1.25	140	177	17.7	82.3
0.65	496	673	67.6	32.4
0.3	280	953	95.3	4.7
0.16	38	991	99.1	0.9
Pan	9	1000	100	0

3.3 Details of Test Specimens

The experimental program comprised 14 large-scale beams of span (L) = 1800 mm, depth (t_b) = 300 mm, and width (b) = 120 mm. The effective depth for all specimens was 260 mm. The beams were simply supported and tested under the effect of four-point bending. The main four variables were the volume of the PVA fibres (0, 0.75%, 1.5%, 2.25%), variable shear span-to-depth ratio, a/d (2.25, 1.5) and variable distribution of stirrups (5Φ6/m, 7.5Φ6/m, 10Φ6/m). The test beams represented four Groups A, B, C, D, and E as indicated in Table 7. All beams were designed according to ECP 203–2007 [24] to be very strong in flexure and very weak in shear to assess the PVA fibre effect on shear behaviour. The steel bars were tied with the stirrups forming reinforcement cages as shown in Fig. 2. Electrical strain gauges of 10 mms length and 120.3 ± 0.5-Ω resistance were fixed on the steel bars, with the positions shown in Fig. 3 to follow the reinforcement strains during loading. The strain gauges were covered with silicon sealant to protect them during casting and consolidation of concrete.

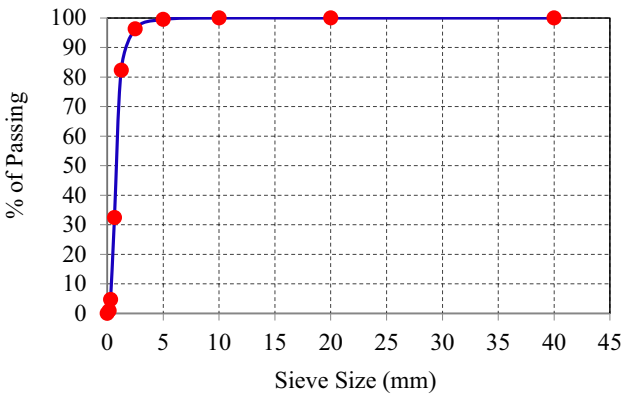

Fig. 1 Sieve analysis curve of the fine aggregate

Table 6 Mix proportions for mortars (Kg/m^3)

Mix	Cement	Fly ash (55%)	Silica fume (15%)	Fine sand	Water	PVA Fibres		HRWR
						(Kg)	%	
1	360	660	180	960	400	0	0.0	11
2	360	660	180	960	400	10	0.75	11
3	360	660	180	960	400	20	1.50	13
4	360	660	180	960	400	33	2.25	15

The mechanical property specimens consisted of twelve cube specimens (100 mm each side) form each mix to test the compressive strength at different ages (three cubes from each mix were tested at 7, 28, 56 and 90 days). In addition, three cylindrical specimens (100 diameter and 200 mm height) for prepared from each mix to test the splitting tensile strength at 90 days. Moreover, three cylindrical specimens were prepared to obtain compressive stress–strain relationships per mix, and to calculate the Young's modulus at the age of 90 days. Therefore, six cylinders were prepared from each mix.

Table 7 Details of the tested beams

Group	Beam	Shear span to depth ratio (a/d)	PVA, V_f %	Stirrups	Mix
A	B1	2.5	0.00	–	1
	B2		0.75	–	2
	B3		1.50	–	3
	B4		2.25	–	4
B	B5	1.5	0.00	–	1
	B6		0.75	–	2
	B7		1.50	–	3
	B8		2.25	–	4
C	B9	2.25	1.50	5Φ6/m	3
	B10		1.50	7.5 Φ 6/m	3
	B11	2.25	1.50	10 Φ 6/m	3
d	12		0.75	5 Φ 6/m	2
	13		0.75	7.5 Φ 6/m	2
	14		0.75	10 Φ 6/m	2
e	15	2.25	0.00	5 Φ 6/m	1
	16		0.00	7.5 Φ 6/m	1
	17		0.00	10 Φ 6/m	1

3.4 Testing of Specimens

At the day of testing, the beam specimen was mounted and adjusted in the loading frame. The beams were loaded in increments up to failure. They were instrumented to measure their deformational behavior after each load increment. Test setup is shown in Fig. 4. The recorded measurements include concrete, longitudinal reinforcement and stirrups strain, lateral deflection and crack propagation. The reinforcement strains were measured using the electrical strain gauges (extensometer) of 10 mm gauge length attached to longitudinal reinforcement and stirrups as shown in Fig. 3. The electrical strain gauges were coupled to a strain indictor. The deflections were measured using three Linear Variable Displacement Transducers (LVDT) 100 mm capacity and 0.01 mm accuracy and arranged to measure the deflection distribution to the specimen as shown in Fig. 3. After each load increment, the cracks were traced and marked on the painted sides of the specimen according to their priority of occurrence.

Fig. 2 Steel reinforcement cages for typical specimens

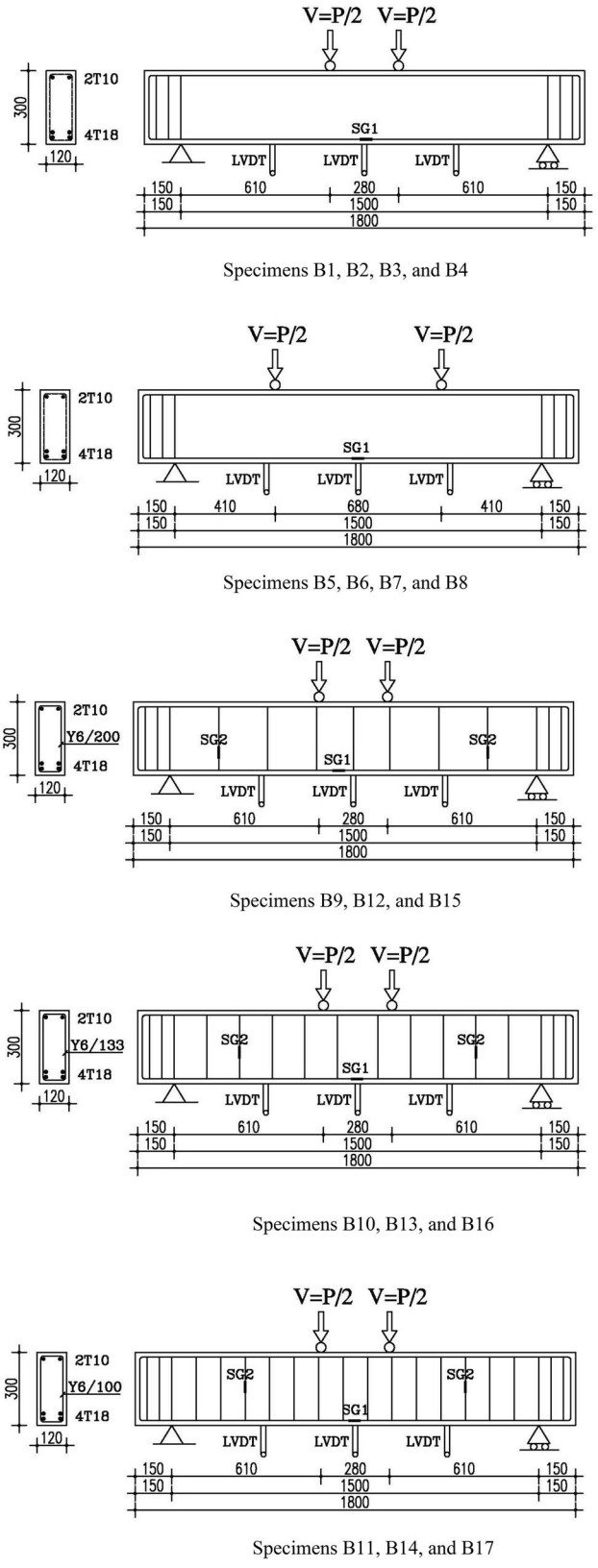

Fig. 3 Position of demec points, electrical strain gauges, and LVDTs

Fig. 4 Test setup for a typical beam

The tests for the mechanical properties of the samples were conducted using a 2000 KN capacity universal testing machine. The compressive and indirect tensile samples were tested to failure. Tests for the stress–strain relationship and Young's modulus were under deformation control with a displacement rate of 0.05 mm/min, in which cylinders were loaded up to 40% of the expected ultimate load. Details of the mechanical testing properties are reported elsewhere [26].

4 Experimental Results and Discussion

4.1 Mechanical Properties for Test Specimens

Table 8 shows the average values (from the three samples tested for each mix) of the mechanical properties for the PVA-mortar mixes. The experimental stress–strain curves for the mixes are presented in Fig. 5. It can be seen from Table 8 that the compressive strength and Young's modulus values were similar for all the mixes. However, the

Table 8 Average test results of compressive, splitting tensile strength, and Young's modulus

Compressive strength (MPa)						
Mix	7 days	28 days	56 days	90 days	Splitting tensile strength (MPa) at 90 days	Young's Modulus (GPa) at 90 days
1	24	44	49	58	5.9	17.3
2	26	45	48	58	8.0	17.8
3	25	44	47	57	10.0	17.6
4	23	43	46	55	13.0	17.5

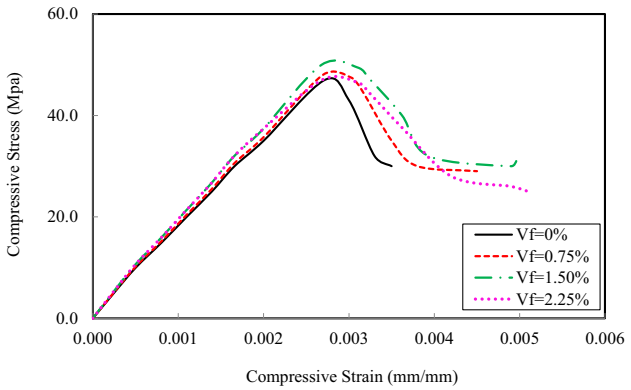

Fig. 5 Compressive stress–strain curves of the mixes

effect of PVA on splitting tensile strength was highly significant, increasing with the increase of PVA content in the mix. For example, the specimens of V_f = 2.25%, 1.5%, 0.75% were higher than that of mortar specimens with no PVA by 160%, 100%, and 60%, respectively. The stress–stain curves in Fig. 5, also show a similar trend as the maximum compressive strength on the curves was only slightly affected by PVA content (ranging between 46 and 49.5 MPa for all mixes), but the ductility increased with increasing the percentage of PVA. This can be indicated by a higher strain at failure, i.e. higher maximum strain, and larger area under the stress–strain curves as seen in Fig. 9. Samples with 2.25%, 1.5%, 0.75% and 0% PVA, had ultimate strains of 0.0051, 0.0049, 0.0045 and 0.0035, respectively. Hence, the maximum strain of specimens of V_f = 2.25%, 1.5%, 0.75% were higher than that of mortar specimens with no PVA by 46%, 40%, and 29%, respectively. The order of magnitude of the values agrees with the results of Meng et al. [26] who reported that the average cylinder compressive strength results of nine PVA-mortar cylinders was 48.4 MPa and corresponding strains were in the order of 0.0055, whereas the average Young's modulus of the PVA-mortar samples was 18.1 GPa.

4.2 Crack Patterns and Failure Mode

All cracks were outlined and labelled at each loading stage with a black marker and crack width was measured using crack measuring scale. Figure 6a–e show the crack pattern and failure modes of all the test beams while the first flexural crack, shear crack, ultimate loads, deflections, and energy absorption which representing ductility are recorded in Table 9.

4.2.1 Group A

Crack pattern and failure modes of beams comprising Group A of *a/d* equals 2.25, and no stirrups, B1, B2, B3, and B4 are shown in Fig. 6a. It can be seen from the figure and Table 9 that B1, with no PVA fibres, had the first flexural cracking load at 22 kN, then shear cracks started at

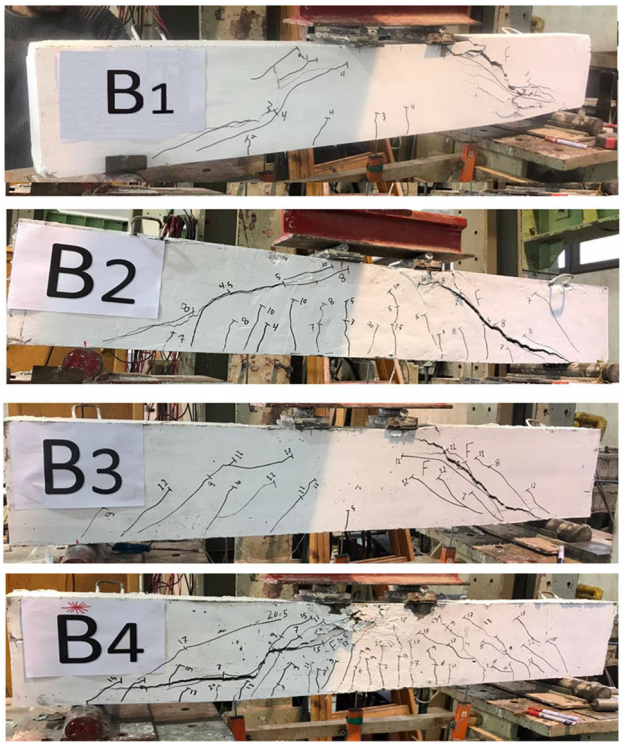

(a) Group A

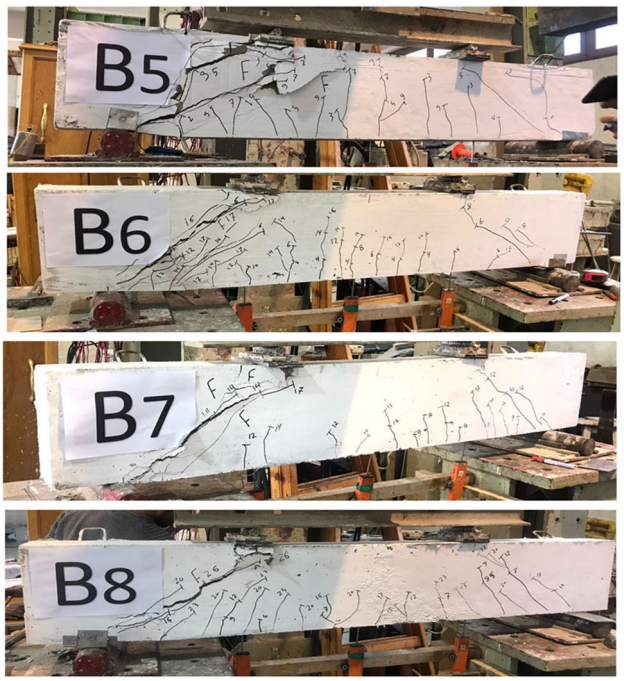

(b) Group B

Fig. 6 Crack patterns and failure modes of experimentally tested beams

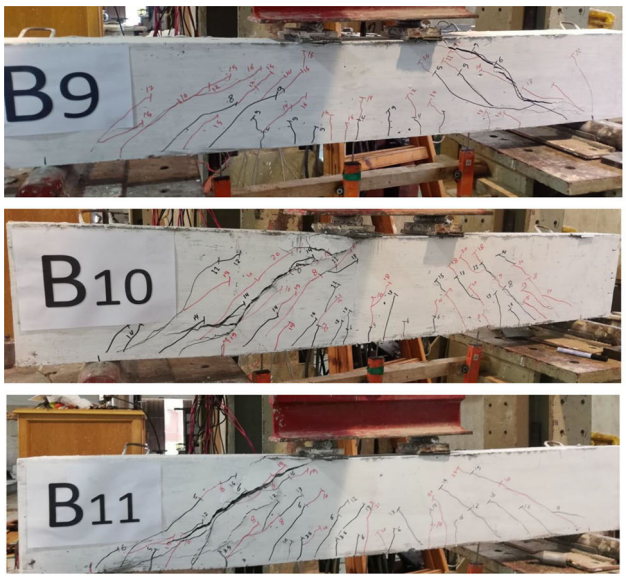

(c) Group C

(d) Group D

Fig. 6 continued

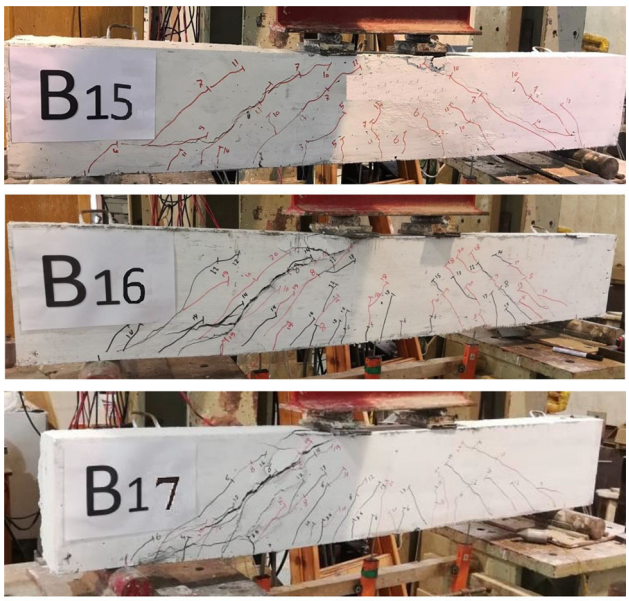

(e) Group E

Fig. 6 continued

27 kN, and the beam failure was brittle in a large diagonal shear crack at ultimate load of 89.5 kN. For B2 including 0.75% PVA, the first flexural crack started at 32 kN, the shear cracks started at 38 kN, and the failure was in a large diagonal shear crack at 134 kN. Increasing the PVA% to 1.5 for B3, led to raising the first flexural cracking load to 40 kN with more flexural cracks as warnings, the shear loads raised to 50 kN, and the failure was also shear at higher ultimate load, 170 kN. A further increase of the PVA% to 2.25% led to a higher first crack load, 48 kN, higher shear crack load, 60 kN, and the failure was due to diagonal shear at 203.3 kN after several warnings of many flexural cracks indicating the ductile behaviour of the beam as can be observed from the increase in the energy absorption.

4.2.2 Group B

Group B specimens of *a/d* equals 1.5, and no stirrups, B5, B6, B7, and B8 had crack patterns and failure modes as shown in Fig. 6b. It can be noticed from the figure and Table 9 that, generally, reducing *a/d* for Group B specimens led to higher first crack flexural, shear loads, and higher ultimate loads compared to those of Group A specimens without changing the mode of failure. For example, B5 had a first vertical crack at 31 KN which is higher than that of B1 by 41%, and the failure was shear at diagonal cracking load from the load application to the support at 95.4 kN. With adding PVA 0.75%, B6, started first vertical flexural crack at 47 kN which is higher than that of B2 by 47%, and new flexural cracks were formed all over the beam with the increment of loading. With further increase in load, existing flexural cracks started to propagate diagonally towards the loading point as well as new diagonal cracks initiated separately away from the mid-span along the beam at 148 kN. Increasing PVA% to 1.5%, B7 behaved as B6 but with higher first crack vertical flexural loads to 57 kN which is higher than that of B3 by 42.5%, and ultimate load to 232 kN. With a further increase of PVA to 2.25%, B8 had a higher first vertical flexural crack of 68 kN which is higher than that of B4 by

Table 9 Comparison between experimental and NLFEA results

Group	Beam	Experimental results					NLFEA results					Experimental /NLFEA Results		
		$P_{cr,\ (flexural)}$ kN	$P_{cr,\ (shear)}$ kN	P_u, kN	δu, (mm)	I^*	$P_{cr,\ (flexural)}$ kN	$P_{cr,\ (shear)}$ kN	P_u, kN	δu, (mm)	I^*	P_u	δu, (mm)	I^*
Group A	B1	22.0	27.0	89.5	3.0	161.0	18.0	20.0	82	3.1	145	1.091	0.955	1.110
	B2	32.0	38.0	134.3	3.7	285.0	25.0	30.0	138.75	3.76	279	0.968	0.987	1.022
	B3	40.0	50.0	170.0	3.92	363.0	31.0	38.0	176	4.3	384	0.966	0.917	0.945
	B4	48.0	60.0	203.3	4.4	504.0	36.0	49.0	203	5	540	1.002	0.880	0.933
Group B	B5	31.0	30.0	95.4	2.5	155.0	26.0	23.0	98	2.4	142	0.973	1.021	1.092
	B6	47.0	40.0	148.0	2.8	246.0	35.0	31.0	142	2.7	210	1.042	1.019	1.171
	B7	57.0	52.0	232.0	3.7	531.0	45.0	44.0	218	3.76	450	1.064	0.976	1.180
	B8	68.0	65.0	264.0	4.3	721.0	55.0	53.0	261	4.26	630	1.011	1.012	1.144
Group C	B9	46.0	60.0	189.0	4.1	500.0	35.0	45.0	181.5	3.98	416	1.041	1.030	1.202
	B10	50.0	60.0	201.0	4.2	552.0	35.0	52.0	183.5	3.88	450	1.094	1.075	1.227
	B11	50.0	70.0	234.5	4.22	617.0	40.0	56.0	219	3.92	510	1.071	1.07	1.210
Group D	B12	40.0	50.0	163.3	4.2	481.0	28.0	38.0	178	4.19	410	0.919	1.012	1.173
	B13	40.0	60.0	173.1	4.2	484.0	34.0	44.0	190.5	4.26	440	0.909	0.986	1.100
	B14	45.0	60.0	200.0	4.0	528.0	36.0	47.0	183	3.92	480	1.095	1.015	1.100
Group E	B15	33.0	48.0	118.0	3.2	250.0	27.0	38.0	128	2.9	215	0.921	1.103	1.160
	B16	35.0	55.0	138.0	3.6	320.0	29.0	42.0	155	3.3	280	0.890	1.090	1.143
	B17	39.0	55.0	170.0	3.7	510.0	32.0	46.0	181	3.55	450	0.939	1.042	1.133

I^* energy absorption

42% and showed many small flexural cracks until the final diagonal shear cracking at ultimate load of 263.8 kN.

4.2.3 Group C

Crack pattern, failure modes, and values of first cracks and ultimate loads of Group C specimens B9, B10, and B11 with *a/d* equals 2.25, PVA of 1.5%, and variable stirrups distribution are shown in Fig. 6c and recorded in Table 9. It can be seen from the figure and the table that the combination of stirrups and PVA in test beams led to a more ductile behaviour compared to their companions in Group A with the same *a/d*, the same PVA content and without stirrups. This can be observed from the increase of energy absorption values of Group C specimens compared with those of Group A ones. This was indicated by more vertical flexural cracks as shown in Fig. 6c and higher first crack flexural and shear loads. For example, B9 with 5Φ6/m stirrups had a first flexural crack load, first shear crack load and ultimate load of 46 kN, 60 kN, and 189 kN which are higher than those of B3 by 15%, 20%, and 11%, respectively. In addition, B10 with 7.5Φ6/m stirrups had a first flexural crack load, first shear crack load and ultimate load of 50 kN, 60 kN, and 200.8 kN which are higher than those of B3 by 25%, 20%, and 18%, respectively. Moreover, for B11 with 10Φ6/m stirrups and PVA of 1.5%, the first flexural crack load, first shear crack load and ultimate load were 50 kN, 70 kN, and 234.5 kN which are higher than those of B3 by 25%, 40%, and 38%, respectively. All the beams in Group C failed in shear with a diagonal shear cracks similar to those in Group A but with a ductile behaviour in terms of several flexural cracks all over the beams as warnings prior to the large diagonal shear cracks at failure.

4.2.4 Group D

Beam specimens of Group D, B12, B13, and B14 with *a/d* equals 2.25, PVAof 0.75%, and variable distribution of stirrups had crack patterns, failure modes, values of first cracks, and ultimate loads as shown in Fig. 6d and recorded in Table 9. It can be seen from the figure and the recorded values in the table that B12 with stirrups 5Φ6/m had first crack flexural load, first shear crack, and ultimate loads higher than those of its companion in Group A, B2 without stirrups by 25%, 32%, and 22%, respectively. In addition Fig. 6d shows that B12 had the dominance of dense flexural cracks noticed until failure compared with specimen B2 (Group A) in Fig. 6b which showed less flexural cracks. On the other hand, B13 with stirrups 7.5Φ6/m had first flexural crack load, first crack shear load and ultimate load of 40, 60, and 173.1 kN which are almost similar to those of Group A, B3, without stirrups and 1.5% PVA. It is interesting to notice that B14 with 10Φ6/m

stirrups and 0.75% PVA shows almost same trend of crack pattern and recorded values of first vertical flexural crack load, first shear crack load and ultimate load almost the same as B4 (Group A) without stirrups and 2.25% PVA.

4.2.5 Group E

For Group E beam specimens B15, B16, and B17 of $a/d = 2.25$ with stirrups only, the crack pattern, failure modes, values of first cracks and ultimate loads are shown in Fig. 6e and recorded in Table 9. It can be seen from the figure and the table that the specimens without PVA showed less ductility compared to the specimens in Groups C and D which have the same *a/d* and contain both of PVA and stirrups. This is observed in the values of energy absorption of these specimens in Table 9. This was indicated by less vertical flexural cracks as shown in Fig. 6e and lower first crack flexural and shear loads. For example, B15 with 5Φ6/m stirrups and no PVA had a first flexural crack load, first shear crack load and ultimate load of 33 kN, 48 kN, and 118 kN which are lower than those of B12 with the same stirrups reinforcement and containing 0.75% PVA by 18%, 4%, and 28%, respectively. In addition, B16 with 7.5Φ6/m stirrups had a first flexural crack load, first shear crack load and ultimate load of 35 kN, 55 kN, and 138.0 kN which are lower than those of B13 which contains 0.75% and the same stirrups reinforcement by 13%, 8%, and 20%, respectively. Moreover, for B17 with 10Φ6/m stirrups, the first flexural crack load, first shear crack load and ultimate load were 39 kN, 55 kN, and 170 kN which are lower than those of B14 of the same stirrups reinforcement and 0.75% PVA by 13%, 8%, and 15%, respectively. Again, all the beams in Group E failed in shear with a diagonal shear cracks similar to those in Group A but the stirrups reinforcement added a ductile behaviour especially for PVA of 0.75, and 1.5%. This was indicated by several flexural cracks all over the beams as warnings prior to the large diagonal shear cracks at failure.

It was observed that during load application, vertical flexural cracks were first observed for all the groups except Group B of *a/d* equals 1.5. These cracks were initiated at the mid-span of all beams as expected. However, the number and width of these cracks differ with variables such as PVA inclusion and content, shear span to depth ratio, and stirrups existence and distribution. All beams failed in shear as they were designed according to ECP 203-2007 [24] to be very strong in flexure and very weak in shear to assess the PVA fibre effect. Failure took place shortly after dominant diagonal shear crack (within one shear span) extended to the top fibre as shown in Fig. 6a–e. The angle of inclination of the diagonal cracks ranged between 30° and 40°. It is interesting to notice that the effect of PVA fibres is comparable to the effect of the presence of shear reinforcement or even better on the shear strength of the studied beams. The results recorded in Table 9 and the crack pattern in Fig. 6 show that the behaviour of B3 with 1.5% PVA and no shear reinforcement is comparable to that of B17 with 10Φ6/m stirrups reinforcement and no PVA fibres. Moreover, B4 with 2.25% PVA and no stirrups showed higher first cracking loads and ultimate loads than those of B17 with 10Φ6/m stirrups and no fibres.

The presence of PVA resulted in several cracks and warnings before failure. The increase of PVA% resulted in a higher tensile strength and, in turn, a significant improvement in ductility. This agrees with the results of Pan et al. [1] as presented in Table 10. It can also be observed that the contribution of PVA towards increasing shear capacity is similar to that of the stirrups. This agrees with Qudah [27] who reported that PVA was effective in replacing the stirrups reinforcement in mortar composites, where the failure was ductile and was triggered by plastic hinging in the beams. It is worth mentioning that for Group B specimens of less *a/d*, beams had a first shear cracking load that is slightly less than the first flexural vertical cracking load, while the opposite was true for Group "A" specimens. In addition, specimen B8 with the maximum PVA, 2.25% showed the maximum ultimate load prior to shear failure. Crack pattern of PVA-mortar beams were similar to that observed by Hasib et al. [28] who studied the shear resistance of composite beams made of two layers, one layer of reinforced concrete and another layer of PVA-mortar without shear reinforcement. They found that PVA-

Table 10 Comparing the inclusion of PVA fibres on the behavior of Beams with Ordinary Mortar Beams in the present work and Pan et al. [1]

Pan et al. [1]			Present Work		
Fibre content (PVA) V_f %	Enhancement in load-carrying capacity	Enhancement in the Tensile strength	Fibre content (PVA) V_f %	Enhancement in load-carrying capacity %	Enhancement in ductility %
M14—0.0%	1.00	1.00	B1—0.0%	1.00	1.00
M15—1.20%	1.00	1.51	B2—0.75%	1.72	1.36
M8—1.30	1.40	1.58	B3—1.50%	2.18	1.69
M16—1.40	1.47	1.78	B4—2.25%	2.61	2.20
M20—1.60	1.57	2.33			

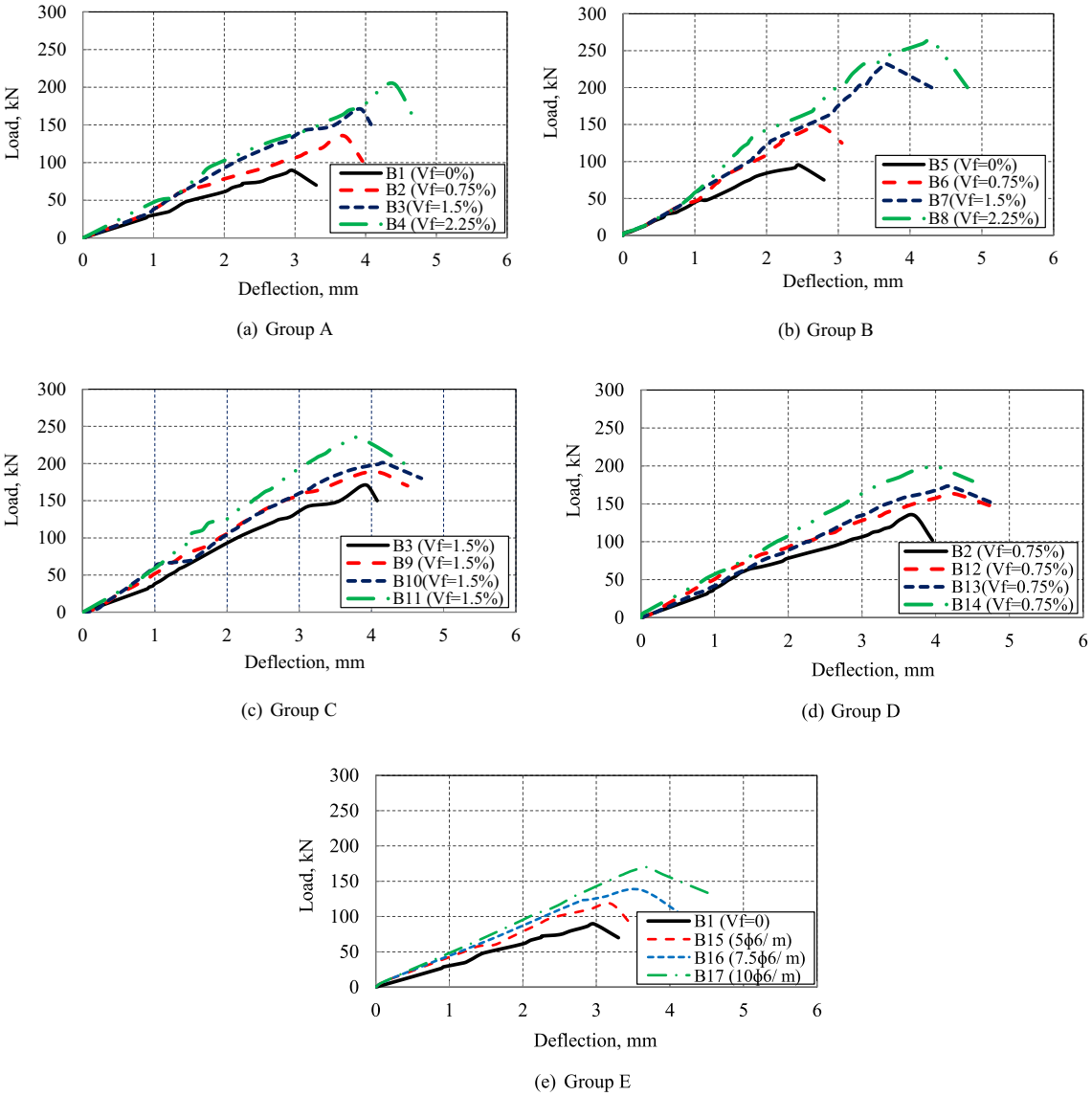

Fig. 7 Load–deflection curves for experimentally tested beams

mortar beams are superior in flexure and shear compared normal reinforced concrete beams without PVA [26]. The minimum increase in the ultimate load as a result of adding PVA in the current study was 50% (B2) higher than that for beams without PVA (B1), while the increase in the ultimate load in PVA-mortar beams of Meng et al. [26] was 14.3% only over that of reinforced concrete beams without PVA. This may be attributed to the effect of adding silica fume to the binder in the current study.

4.3 Load–Deflection Relationships

Figure 7a–e shows the load–deflection relationships for the test specimens comprising the five studied groups mentioned in Table 7. It can be seen from the figures that, generally, the load displacement for all the test specimens exhibited similar pattern for the different studied groups but with different ultimate loads and corresponding deflections, based on the studied variables, namely *a*/*d*, PVA%, and presence of stirrups.

4.3.1 Group A

For Group "A" specimens tested at *a*/*d* equals 2.25, Fig. 7 a shows that adding PVA to the mix resulted in a significant improvement in the performance of the studied beams compared with the control one without PVA. This is indicated by an increase in the ultimate load, and corresponding deflection. In addition, increasing the percentage of PVA resulted in a further improvement in the

performance. For example, specimen B1 with no PVA had an ultimate load and corresponding deflection of 89.5 kN, and 3 mm, respectively. For specimens B2 with PVA% equals 0.75%, B3 with PVA% equals 1.5% and B4 with PVA% equals 2.25%, the ultimate loads were higher than that of specimen B1 by 50%, 92% and 157%, and their corresponding deflections were higher than that of specimen B1 by 24%, 31%, and 47.3%, respectively.

4.3.2 Group B

The load–deflection curves for Group "B" specimens tested at *a/d* equals 1.5 are shown in Fig. 7b. It can be seen from the figure that generally, the specimens of *a/d* equals 1.5 showed higher ultimate loads compared with those of specimens of higher *a/d* (2.25) shown in Fig. 7a. For example, Fig. 7b shows that Specimen B5 without PVA had an ultimate load of 95.35 kN which is higher than that of B1 (Group A) of *a/d* equals 2.25 by 7%. Figure 7b shows also that specimens B6 with PVA% equals 0.75%, B7 with PVA% equals 1.5% and B8 with PVA% equals 2.25%, had ultimate loads higher than that of specimen B5 by 55%, 144% and 177%, and their corresponding deflections were higher than that of specimen B5 by 16.3%, 44%, and 75.9%, respectively.

4.3.3 Group C

The load deflection curves of Group "C" specimens of specific content of PVA, 1.5%, presence of stirrups, and *a/d* equals 2.25 are shown in Fig. 7c. It can be seen from the figure that the combined effect of stirrups and PVA resulted in a slight improvement in the performance of studied beams compared with that of beam B3 which included PVA without stirrups. Figure 7 (c) shows that specimens B9 with stirrups 5ϕ6/m, B10 with stirrups 7.5ϕ 6/m, and B11 with stirrups 10ϕ6/m had ultimate loads higher than that of specimen B3 (Group A) of the same PVA percentage and without stirrups by 17%, 18% and 38% and their corresponding deflections were higher than that of specimen B3 by 5.20%, 7.30%, and 8.50%, respectively.

4.3.4 Group D

Figure 7d shows the load deflection curves for Group "D" specimens with less percentage of PVA, 0.75%, and presence of stirrups. It can be seen from Fig. 7d that generally the ultimate loads are less than those of the specimens with the same stirrups areas and higher PVA, 1.5% in Fig. 7c. It can be seen from Fig. 7d that the ultimate loads and corresponding deflections of the beams including PVA and stirrups are higher than those of B2 with the same PVA percentage and without stirrups. In addition, these values increased with increasing the area of the stirrups. For example, the ultimate loads of specimens B12, B13 and B14 were higher than those of B2 (Group A) without stirrups by 13%, 15% and 31.5%, while their corresponding deflections were higher than those of specimen B2 by 13%, 13%, and 7%, respectively.

4.3.5 Group E

The load–deflection curves for Group "E" specimens with no PVA, and with different stirrups reinforcement distribution are shown in Fig. 7e. It can be seen from the figure that generally the ultimate loads of Group "E" specimens are higher than that of the control beam B1 of Group "A" without fibres and stirrups. In addition, Table 9 shows that the first cracking flexural and shear loads of B15–B17 of Group "E" are almost similar to those of B2 and B3 of Group "A" which contain 075% and 1.5% PVA and no stirrups. Moreover, the first flexural and shear cracking loads of B4 which contains 2.25% PVA and no stirrups was higher than that of B17 of Group "E" with 10ϕ6/m stirrups and no fibres. The ultimate loads of specimens with no shear reinforcement (Group A), B2 (0.75 & PVA), B3 (1.5% PVA) and B4 (2.25% PVA) were higher than those of specimens with no PVA (Group E), B15 (5Φ6/m), B16 (7.5Φ6/m), and B17 (10ϕ6/m) by 12%, 19% and 16%, respectively.

It can be seen from the above results and the curves shown in Fig. 7a–e that the inclusion of PVA fibres led to an increase in the tensile strength of test beams which, in turn, improved shear resistance by raising the cracking loads and ultimate loads compared to beams without PVA as indicated in Table 9. In addition, the combination of PVA fibres and the stirrups (transverse) reinforcement contributed to the shear behaviour of studied beams. Moreover, specimens containing PVA fibres and without shear reinforcement have higher ultimate loads than those with shear reinforcement and without PVA fibres. Comparison of the results showed that the effect of PVA fibres on the ultimate loads (shear capacity) and corresponding deflections was more significant for lower shear span-to-depth ratio (*a/d*) and with reducing the amount of shear reinforcement. Shimizu et al. [29] also showed that the shear strength of steel reinforced PVA-mortar beams increased with the increase in volume percentage of PVA fibre. For beams of *a/d* equals 1.5 and containing PVA equals 2%, Shimizu et al. [29] found that the increase of ultimate load was 80% higher than their companion of normal concrete without PVA, while the beams of the current study of the same *a/d* and containing PVA equals 2.25%, the increase in ultimate load was 177% compared to beams without PVA. This may be attributed to the

combined action of PVA fibres and cement replacement materials, fly ash and silica fume, which formed the mortar composites in the current study.

4.4 Energy Absorption (*I*)

Energy absorption was defined as the area under load–deflection curves and it is a good indication to measure the ductility of structural elements [30]. It can be seen from Fig. 7a–e and Table 9 that, generally, the energy absorption was enhanced by increasing PVA fibre content. In addition, the combination of stirrups and PVA improved the ductility of studied specimens. Moreover, the shear span to depth ratio has a significant effect on the ductility of specimens. The maximum energy absorption was observed for Group B of *a/d* equals 1.5 especially for Specimen B8 where the PVA% equals 2.25% and without stirrups. For example, Fig. 7a and Table 9 show that for Group A with *a/d* equals 2.25 and no stirrups, the energy absorption for specimens B2, B3 and B4 were higher than that of B1 by 77%, 125% and 213%, respectively. With reducing the *a/d* to 1.5, Fig. 7b and Table 9 show that Group B specimens, B6, B7, and B8 had energy absorptions of 59%, 243% and 365% higher than that of specimen B5 without PVA. For Group C with 1.5% PVA and presence of stirrups, Fig. 7c and Table 9 show that the enhancement of energy absorption of specimens B9, B10, and B11was higher than that of specimen B3 of the same content of PVA and without stirrups by 38%, 52%, and 70%, respectively. For Group D specimens with less PVA, 0.75%, and presence of stirrups, Fig. 7d and Table 9 show that the energy absorptions of specimens B12, B13, and B14 were higher than that of B2 by 69%, 70%, and 85%, respectively. For Group E specimens with no PVA and stirrups only, Fig. 7e and Table 9 show that the energy absorptions of B15 and B16 with stirrups only were lower than those of B2 and B3 with PVA fibres only by 12.1% and 11.8%, respectively.

Enhancement of energy absorption was observed for PVA-mortar beams. This implies that the number of stirrups could be reduced when the PVA is added to the mortar matrix in a reasonable percentage (minimum 1.5%). The shear behaviour of beams without stirrups (shear reinforcement) was studied by Ismail and Hassan [13]. They reported that the PVA-mortar beams showed better performance in terms of cracking behaviour, shear capacity, ductility and energy absorption compared with the conventional reinforcement concrete beam. In addition, Hossain et al. [31] reported that PVA-mortar was effective in replacing the stirrups reinforcement and the energy absorption was improved for specimens containing PVA compared with self-consolidating concrete (SCC) beam specimens of *a/d* equals 1.53. They found that the energy absorption for PVA-mortar beams was higher than that for SCC by 100% for beams without stirrups reinforcement, while, in the current study, the energy absorption for PVA-mortar beams of the same *a/d*, B7 with 1.5% PVA was higher than that of B5 with no PVA by 242%. The drastic improvement of the results of PVA-mortar beams in the current study revealed the significance of combining fly ash, silica fume with PVA fibres.

4.5 Load–Strains Relationships

The strains in the longitudinal tension bars and stirrups reinforcement were measured as explained in Sects. 3.3 and 3.4. The load strain relationships for longitudinal bars in studied specimens are shown in Fig. 8a–e and the load strain curves for stirrups are shown in Fig. 9a–c.

4.5.1 Load–Strain Curves for Longitudinal Reinforcement

As was observed previously for the crack pattern and failure modes in Sect. 4.1, all PVA-mortar beams have failed in shear. This was indicated in Fig. 8a–e that the maximum loads recorded for longitudinal tension bars were less than the ultimate shear load at failure, recorded in Table 9, and the corresponding strains were all less than the yield value. For example, it can be seen from Fig. 8a that for Group A specimens, B1, B2, B3, and B4, the maximum load was 195 kN for B4 which is lower than the ultimate shear load recorded in Table 9 (204 kN), while the maximum strain was 0.0009 for B2. Figure 8b shows that the maximum load for B8 of *a/d* equals 1.5 was 240 kN which is lower than ultimate shear load recorded in Table 9 (264 kN) and corresponding strain was 0.00125 which is higher than that for its companion B4 of *a/d* equals 2.25 by 78.6%. On the other hand, Fig. 8c–e show that the maximum load at longitudinal reinforcement are almost the ultimate loads recorded in Table 9 and the corresponding strains of Groups C, D, and E specimens with stirrups are more than double as much those of Groups A and B specimens which indicate the shear failure shown previously in crack pattern and failure modes. For example, Fig. 8c, Group C specimens of PVA (1.5%) had maximum load equals 234 kN and the corresponding strain was 0.0023 for B11 which are higher than those of its companion B3 of the same PVA content without stirrups by 42% and 233%, respectively. In addition, Fig. 8d shows that the maximum load was 200 kN for B14, while maximum strain was 0.0022 for B12 which is higher than that of its companion B2 without stirrups in Group A by 144.4%. Moreover, Fig. 8e shows that the maximum load was 170 kN for B17, while maximum strain was 0.002 for B15 which is higher than the maximum strains of the beams in Group A. This may be attributed to the fact that the presence of stirrups in Groups C, D (in combination with PVA-mortar) and in Group E contributed

to resist shear stresses which led to further action of longitudinal reinforcement in flexure which resulted in higher strains in longitudinal bars.

4.5.2 Load–Strain Curves for Stirrup Reinforcement

Figure 9a–c shows the load–strain relationships for stirrups reinforcement in Groups C, D, and E. It can be seen from the figures that, for all specimens with stirrups, the strains along the stirrups exceeded the yield value. In addition, the maximum loads at stirrups and corresponding strains for specimens in Group C containing PVA equals 1.5% are higher than those of Group D with PVA equals 0.75% and those of Group E without PVA fibres. For example, B9 in Group C had a maximum load of 155 kN and corresponding stirrups strain of 0.0062 which are higher than those of B12 in Group D by 0% and 26.5% and those of B15 in Group E by 24% and 19%, respectively. In addition, B10 in Group C had a maximum load at stirrups of 200 kN and corresponding stirrup strain of 0.0064 which are higher than those of B13 in Group D by 14.3% and 60%, and those of B16 in Group E by 30.5% and 30%, respectively. Moreover, B11 in Group C had a maximum load of 240 kN and corresponding stirrup strain of 0.0059 which are higher than those of B14 in Group D by 20% and 9.2%, and higher than those of B17 in Group E by 29.1% and 17%, respectively. It can be argued that the improvement of ductility of studied beams as a result of the combination of PVA of 1.5% with stirrups was higher than that for the combination of half content of PVA (0.75%) with the same amount of stirrups or their companions with stirrups only. In other words, increasing PVA% resulted in improvement

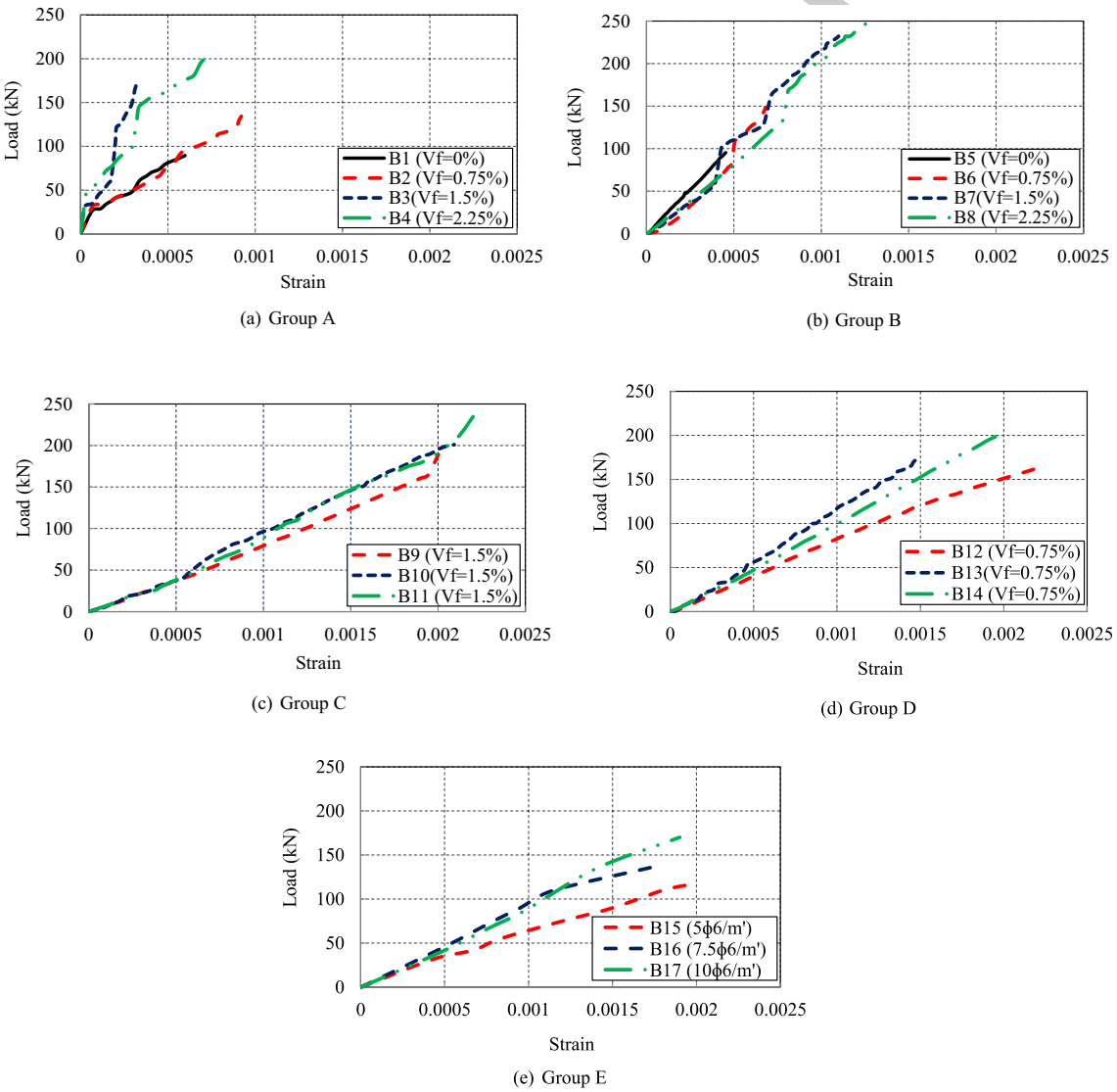

(a) Group A (b) Group B

(c) Group C (d) Group D

(e) Group E

Fig. 8 Load–strain curves for longitudinal reinforcement

of shear strain and this improvement is more significant for beams without stirrups. In their study of the shear behaviour of steel reinforced PVA-mortar beams, Hasib and Hossain [28] reported that the average shear strain in shear crack surface at maximum strength is highly influenced by differences of volume percentage of PVA fibre.

From the above results, the authors recommend a combination of at least 1.5% PVA and stirrups reinforcement (minimum 5Φ6/m) to achieve adequate shear behaviour of PVA-mortar beams. This combination prevented sudden failure and improved the ductility as several small flexural cracks were formed prior to failure. The effect of both of PVA% and transverse reinforcement ratio % on the ultimate loads of the studied beams is shown in Fig. 10. It can be seen that at the same percentage, the PVA has higher effect on the ultimate load compared to that of transverse reinforcement.

5 Non-linear Finite Elements Analysis (NLFEA)

The experimentally tested PVA-reinforced mortar beams were modelled using the non-linear finite element package ANSYS 14.5 [32] to predict the structural behaviour. The load–deflection relationships and the crack patterns for test beams were conducted to verify the numerical modelling with the obtained experimental results. Based on the ANSYS program manual, the finite element modelling of mortar, PVA fibres, and steel in PVA-reinforced mortar beams are briefly described in the following sections.

5.1 Modeling of Test Beams

In the finite element discretization of each beam, a mesh of average size 25 × 25 × 20 mm of eight-node elements was used for all beams. The area and spacing of bar elements were similar to those used in the experimental specimens. The concentrated loads were also applied to the top surface at mid-span of the tested beams. The supports were represented by restrained nodes at the corresponding locations. The structural element type used for geometric idealization of the mortar is Solid 65 as its capability to the plastic deformation, cracking and crushing in three directions. The PVA fibres were simulated as smeared reinforcements in Solid 65 element represented through volumetric ratio to represent the actual fibre volumes used in each beam specimen [33]. It is defined by eight nodal points as shown in Fig. 11. Stress–strain curves in mortar in compression which are shown in Fig. 5 and the properties of PVA-mortar composites recorded in Table 8 were used in the model.

Longitudinal steel reinforcement and stirrups were modeled using the ANSYS 3D Spar LINK 180 elements as shown in Fig. 12. The element is a uniaxial tension–compression element with three degrees of freedom at each node. The material properties of the steel reinforcement have been obtained from the experimental testing. The steel yield strength, elastic modulus and Poisson's ratio were taken as 450 MPa, 200 GPa and 0.3, respectively. The average stress–strain curve developed earlier [34] for steel bars embedded in concrete is used in the current research (see Fig. 13). The stress–strain relationship is expressed by two straight lines and the non-linear behaviour of steel was

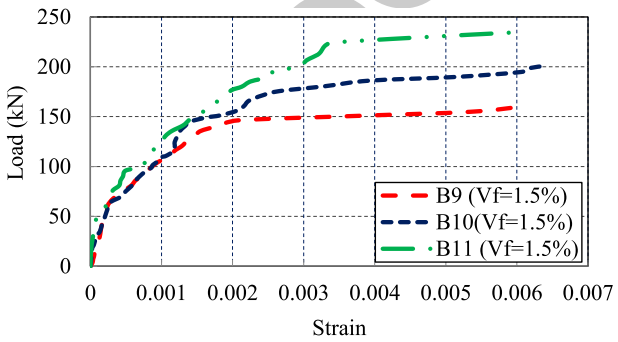

(a) Group C

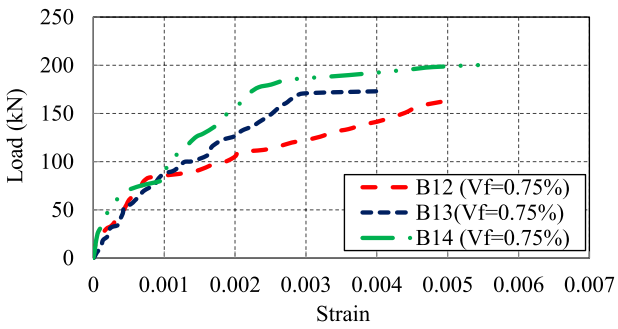

(b) Group D

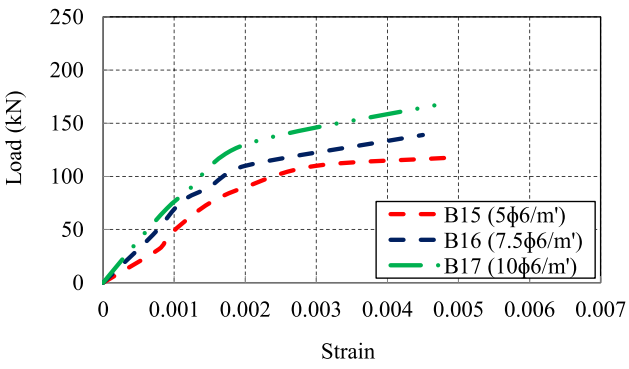

(c) Group E

Fig. 9 Load–strain curves for stirrups

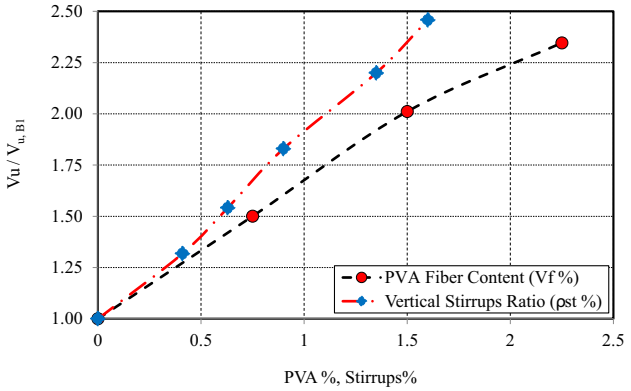

Fig. 10 Effect of PVA-Fiber content (V_f %) and transverse reinforcement ratio (ρ_{st} %) on the ultimate capacity of studied beams

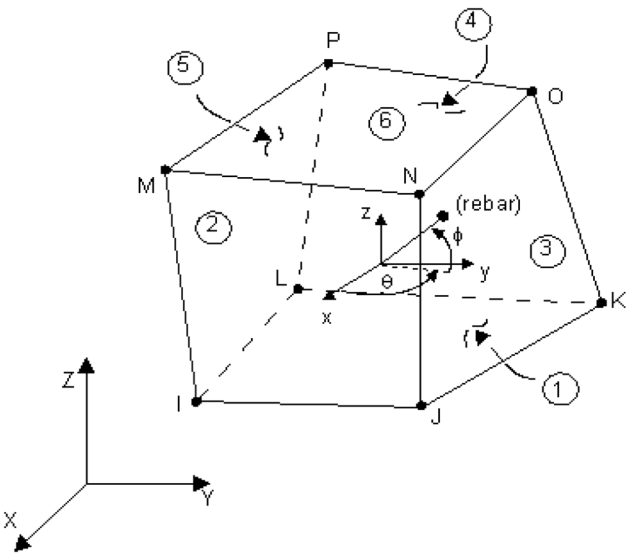

Fig. 11 Geometry of 3-D Solid 65 Element [30]

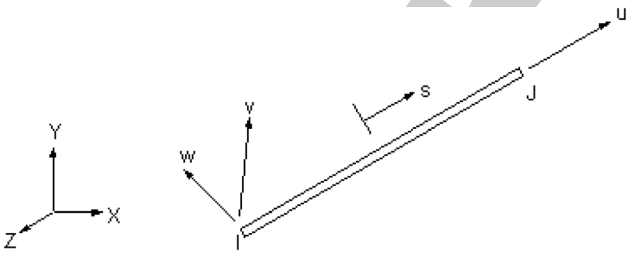

Fig. 12 3-D Spar LINK 180 element [30]

modeled as bilinear. Solid 45 was idealized at the location of loading and supports in the concrete beams to avoid stress concentration problems. Figure 14 shows the typical idealization of the Composite PVA-mortar composites and steel elements for the tested beams used in the analysis.

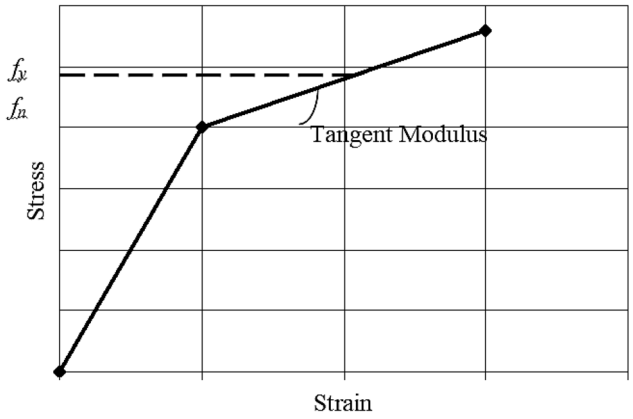

Fig. 13 Stress–strain curve for steel reinforcement [32]

5.2 Prediction of Crack Pattern and Load–Deflection Results

Figure 15 shows the comparison between experimental and predicted crack pattern at failure for typical specimens, namely, B4 and B12. It can be seen from the figure that the developed cracks in the PVA-mortar beam specimens are well distributed through the whole span. The shear stresses increases with increasing the load increment, start to induce diagonal cracks, and the shear failure was recorded. Good agreement was observed between the simulated crack patterns and the obtained experimental ones. The simulation also successfully predicted the sequence in the crack pattern development and the failure mechanism.

Figure 16 shows the numerical load deflection curves for the studied beams compared with the experimental ones for all beam specimens. It can be seen from the figure that, generally, the load–deflection relationships for all specimens exhibited similar features and the predicted load–deflection curves of most of the specimens were very close to the experimental ones. As ANSYS can measure the load–displacement until the failure only [32], its prediction does not show a reduction in the load after reaching the ultimate value compared with the experimentally obtained value. Values of experimental and numerical first crack flexural loads ($P_{cr,\ M}$), first crack shear loads ($P_{cr,\ S}$), ultimate loads (Pu), ultimate displacements (δ_u), and energy absorption (I). In addition, a comparison between predicted and experimental ultimate loads, corresponding displacements and energy absorption of the test specimens is given in Table 9. A very good agreement between the experimental results and the numerical ones was observed. The ratio of the predicted to experimental ultimate loads, corresponding displacements, and energy absorptions ranged between 0.89–1.095, 0.88–1.10, and 0.93–1.22, respectively.

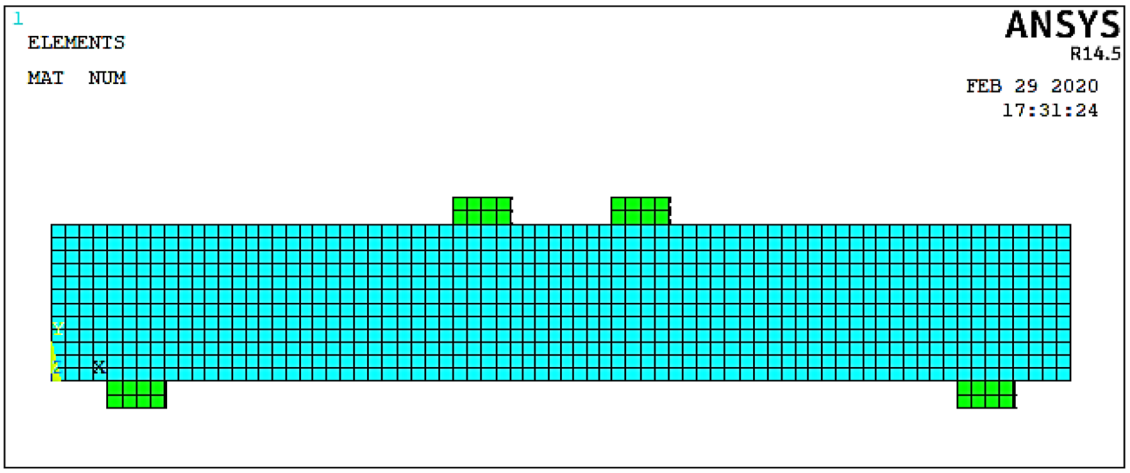

Specimens with a/d= 2.25

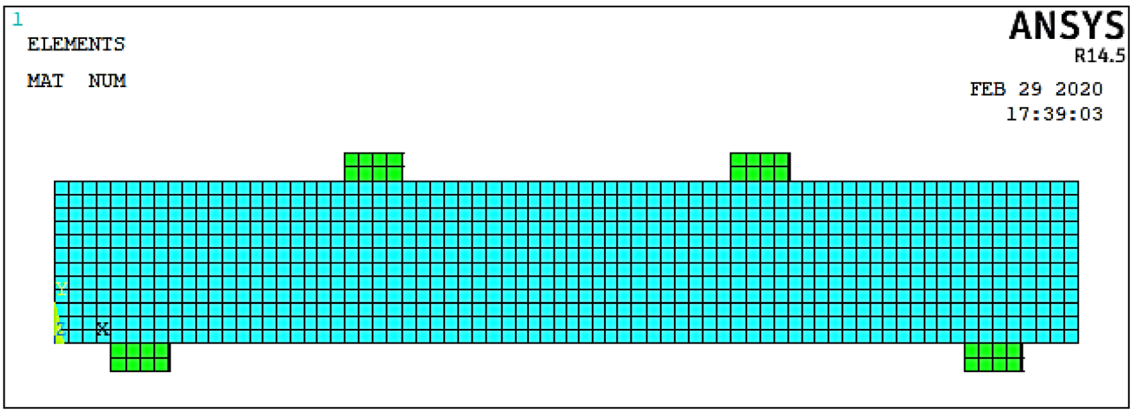

Specimens with a/d= 1.50

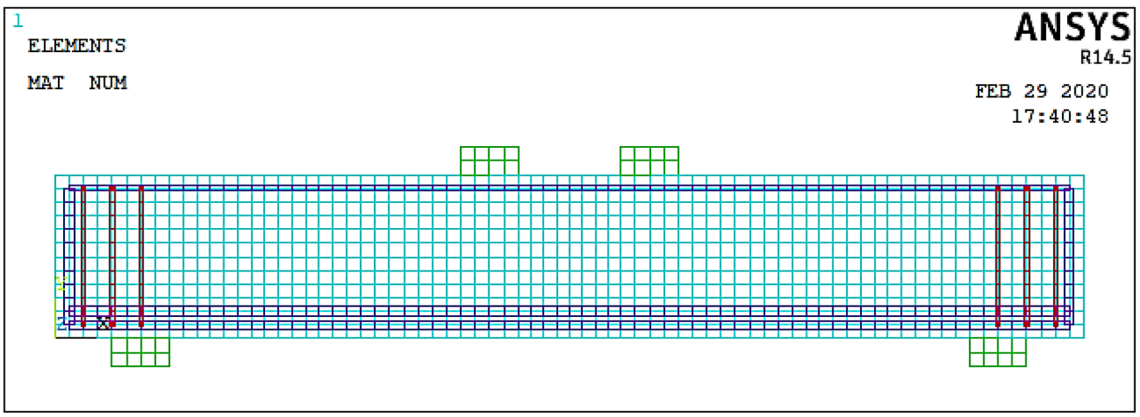

Specimens without Stirrups

Fig. 14 Finite element modeling of test beams

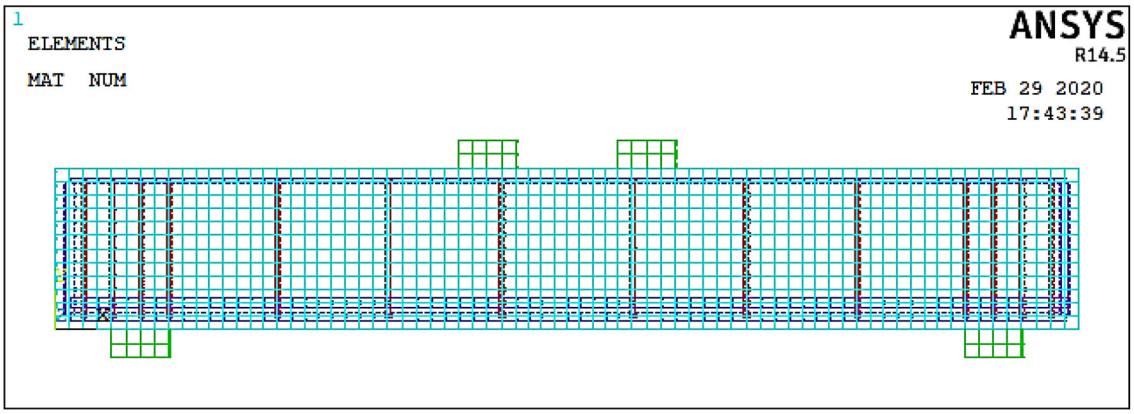

Specimens with Stirrups 5ϕ6/ m’

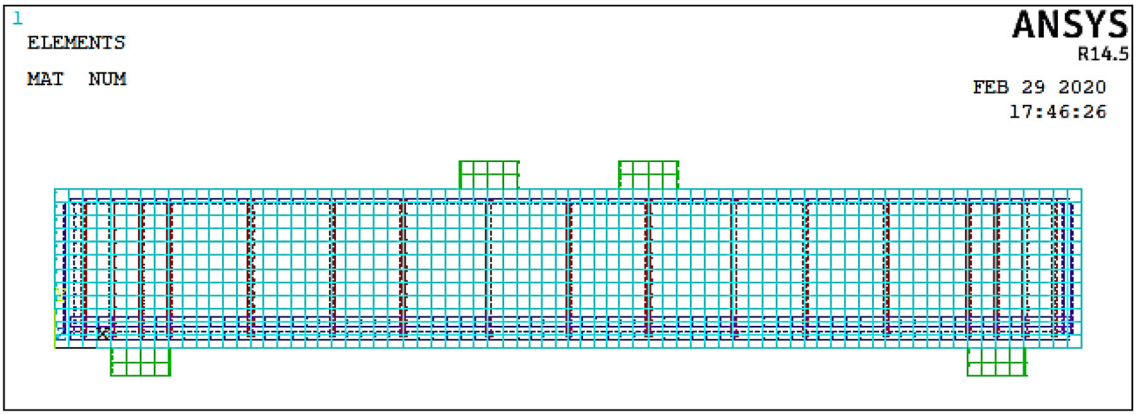

Specimens with Stirrups 7.5ϕ6/ m’

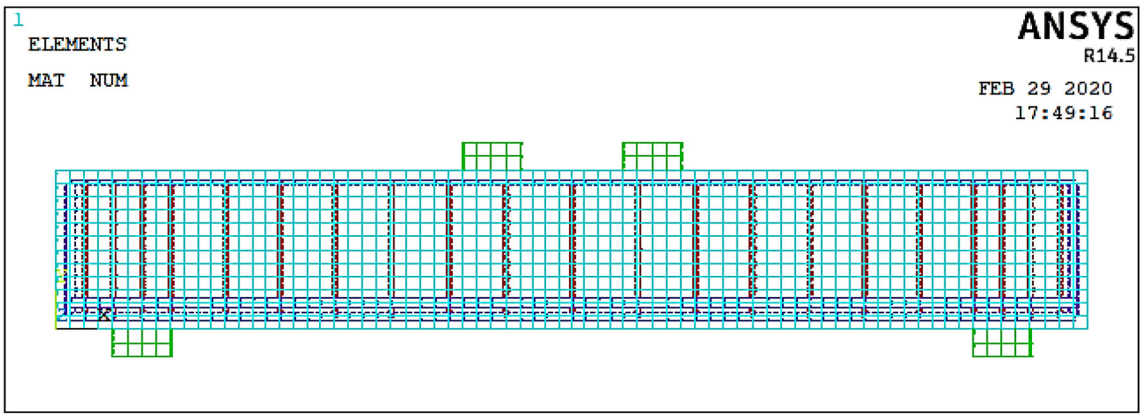

Specimens with Stirrups 10ϕ6/ m’

Fig. 14 continued

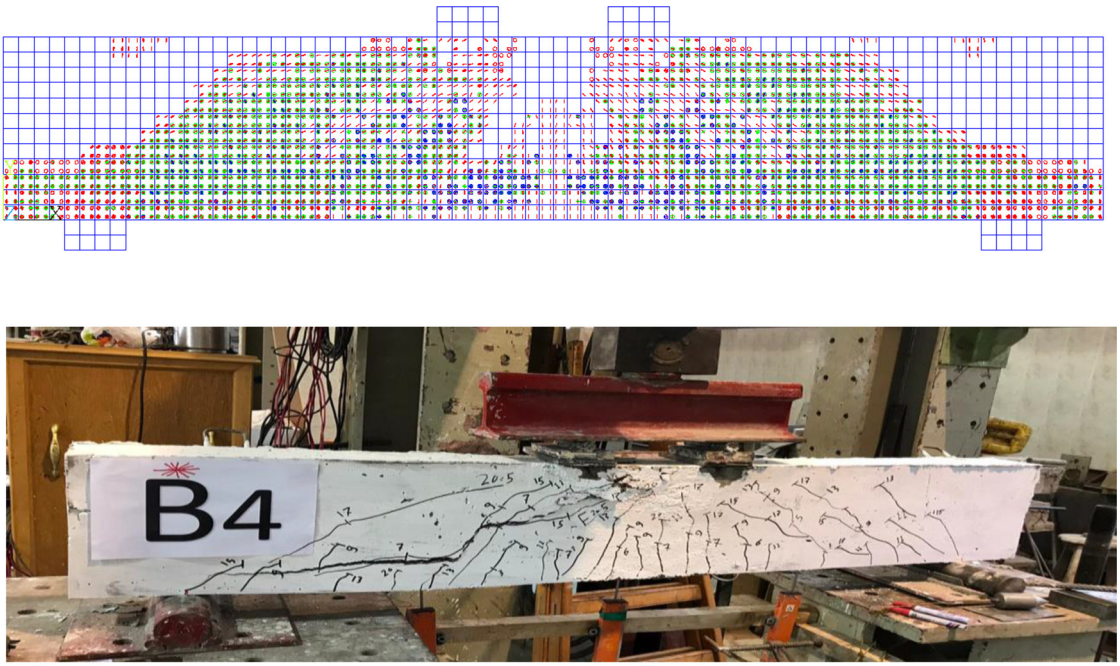

(a) B4

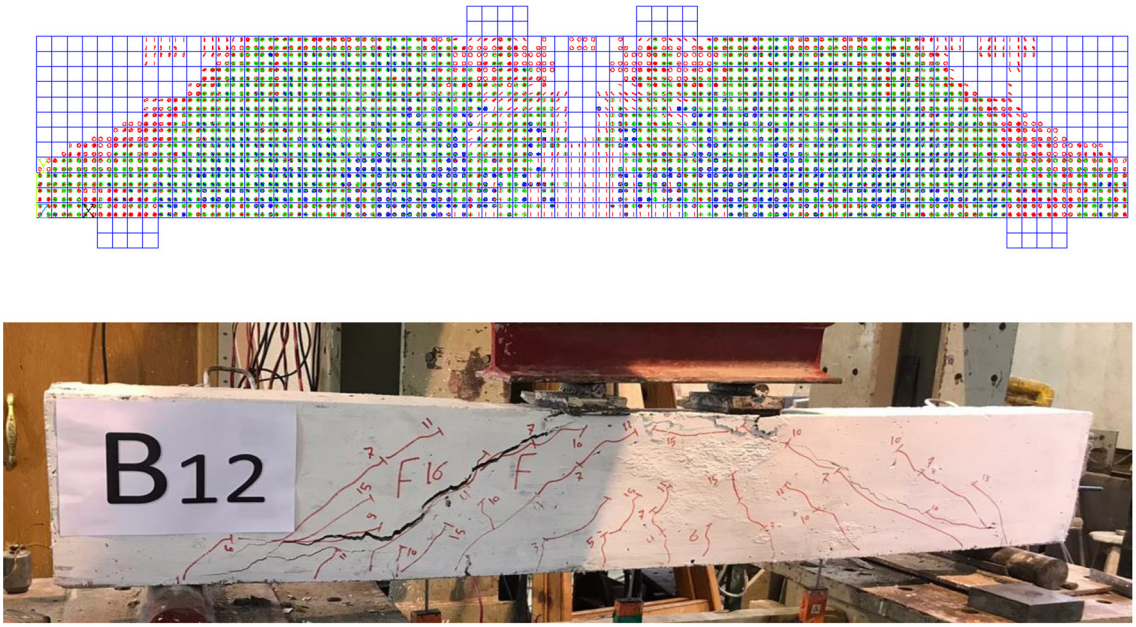

(b) B12

Fig. 15 Predicted crack pattern for selected beams at failure

It can be seen that within the range of the test parameters investigated, the application of the non-linear finite element model, developed in this study, yielded satisfactory first shear and flexural cracking loads, ultimate capacity and deflections, load–deflection relationships, and energy absorptions.

6 Prediction of Ultimate Shear Strength

The predicted analytical ultimate shear strength ($V_{u,\ Anal.}$) for PVA-Mortar beams was performed to be compared with the experimental test results. A proposed equation was developed in the current research which is an enhancement

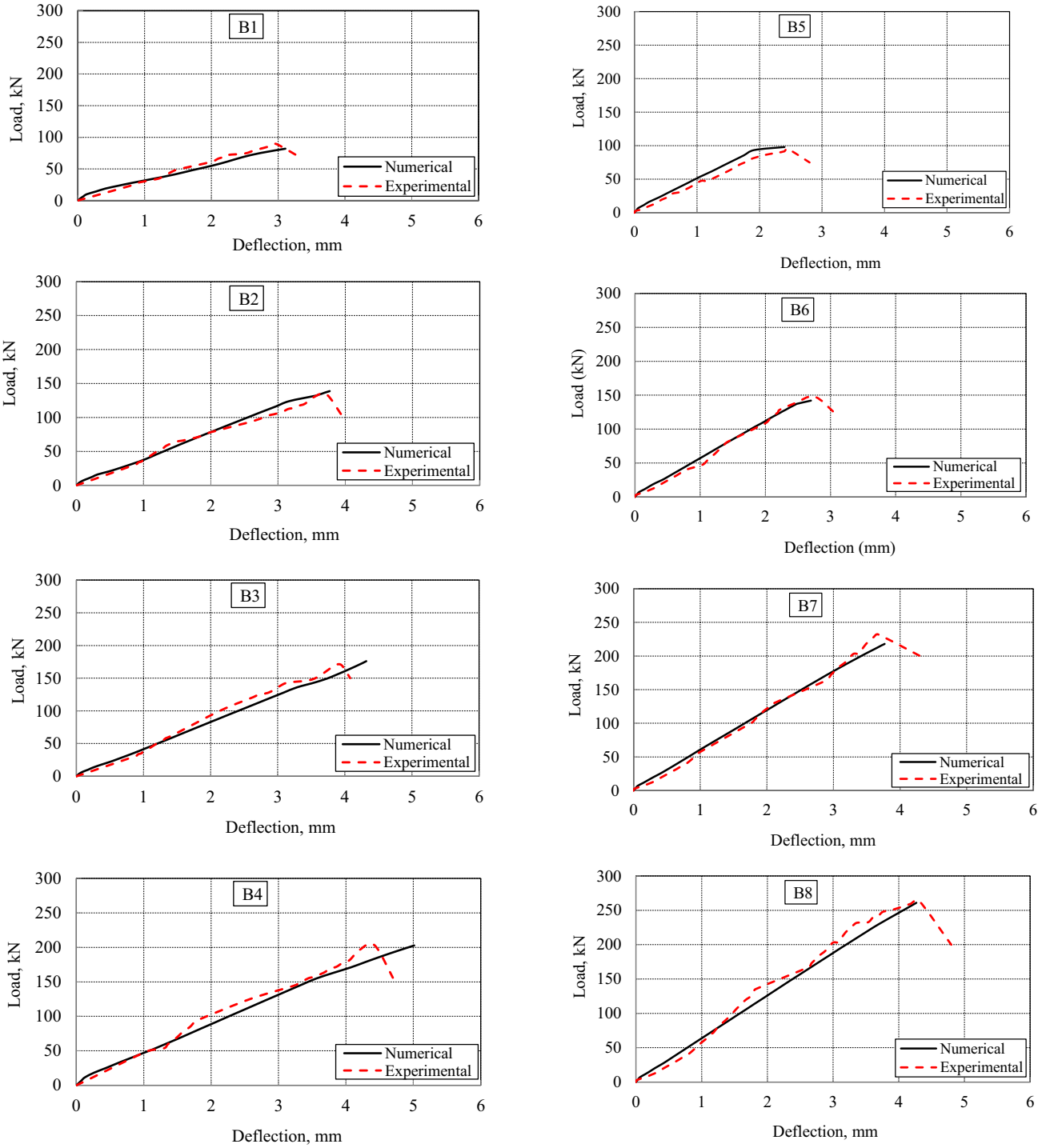

Fig. 16 Finite element prediction of load–deflection curves for test beams

equation of CSA Standard [35]. The ultimate shear strength was predicted for a typical rectangular beam of a cross-section ($b \times t$) as follows:

$$V_{u,Anal.} = V_c + V_f + V_s. \quad (1)$$

The contribution of concrete to the shear resistance (V_c) can be estimated by the empirical equation of CSA Standard [35] as follows:

$$V_c = \left(\Phi_c \lambda \beta \sqrt{f_c'}\right) b d_v, \quad (2)$$

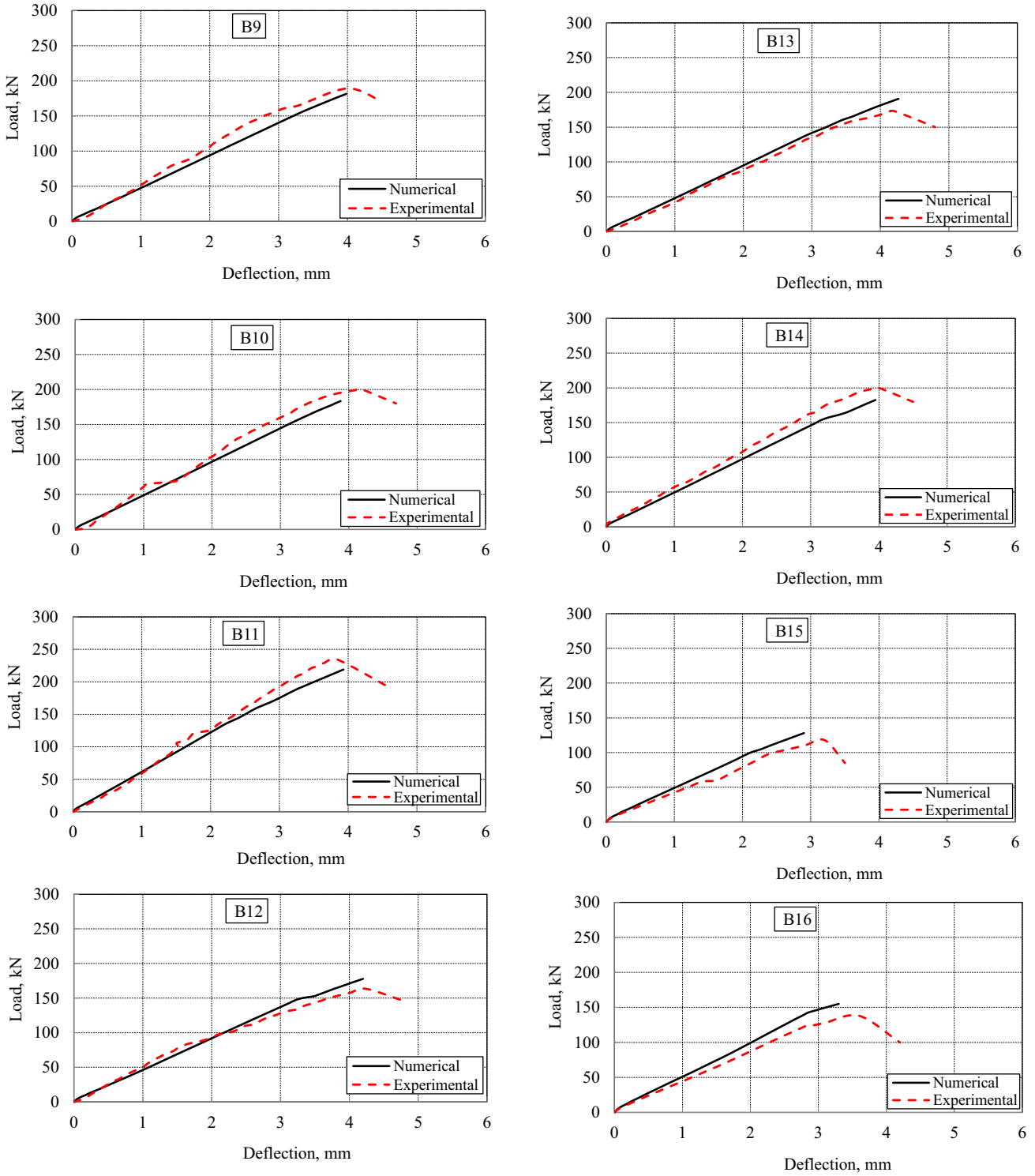

Fig. 16 continued

where the value of the factors ϕ_c, λ, and β are 0.65, 1.0, and 0.21, respectively. In addition, the value of d_v was taken as the maximum of 0.9 the effective depth (d) or 0.75 the section depth (t) [35].

The contribution of PVA fibres to shear resistance (V_f) can be predicted as follows:

$$V_f = F_{PVA}\beta_o\tau b d_v. \quad (3)$$

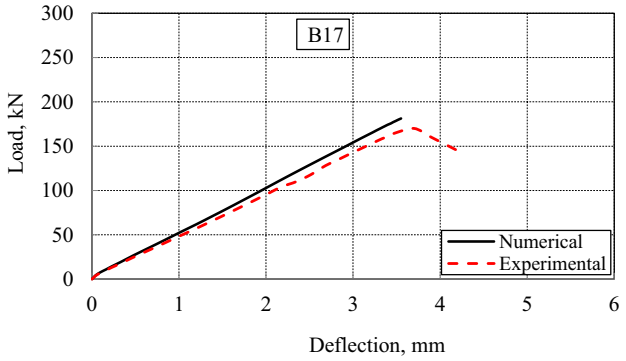

Fig. 16 continued

The fiber factor for PVA fibres (F_{PVA}) is considered as [36]:

$$F_{\mathrm{PVA}} = V_{\mathrm{F,PVA}} \frac{l_{\mathrm{f}}}{\Phi_{\mathrm{f}}} \lambda_{\mathrm{f}}, \tag{4}$$

where ($V_{\mathrm{F,\ PVA}}$) is the percentage volume of PVA fibres, l_{f} is the fiber length (12 mm), ϕ_{f} is the fiber diameter (0.04 mm), ($l_{\mathrm{f}}/\phi_{\mathrm{f}}$) is the PVA fibres aspect ratio, and λ_{f} is the shape factor with value of 0.5 [36]. In addition, the orientation factor (β_{o}) is considered 0.41 [36], and the interface frictional bond of PVA fibres (τ) is taken as 2.93 MPa [37].

The contribution of vertical stirrups in shear (V_{s}) can be defined as follows [35]:

$$V_{\mathrm{s}} = \Phi_{\mathrm{s}} \frac{A_V}{S} f_{\mathrm{ys}} b d_{\mathrm{v}}, \tag{5}$$

where A_{v} is the area of the vertical stirrups, f_{ys} is the yield stress of the stirrups, the value of the factors ϕ_{s} is taken as 0.85, and spacing between the stirrups (S) was variable for the different specimens used in this investigation (B9–B17). Accordingly, the ultimate shear strength ($V_{\mathrm{u,\ Anal.}}$) can be predicted from Eq. (1). The analysis procedure for calculating $V_{\mathrm{u,\ Anal.}}$ can be easily implemented by hand calculations or a spreadsheet. Table 11 presents a comparison between the experimental and predicted ultimate shear strength. Good agreement was achieved between the experimental and predicted shear strength results. The overall average value of the ratio [$V_{\mathrm{u,\ exp.}}/V_{\mathrm{u,\ Anal.}}$] for the studied beams is 1.038 with a standard deviation of 0.11 and the coefficient of variation equals 10.50%.

7 Conclusions

The current study aimed to investigate the shear behaviour of PVA-mortar beams. The studied variables were different percentages of PVA fibres (0.75%, 1.5%, and 2.25%), shear span to depth ratio (a/d = 1.5, and 2.25), and stirrups reinforcement ratio (5Φ6, 7.5Φ6, and 10Φ6/m'). Fourteen PVA-mortar beams were experimentally tested. Predictions of the results were carried out using a rational empirical arch-truss approach. The following conclusions were drawn from this study.

Failure modes of all the test beams were in shear. However, the addition of PVA had a significant effect on the crack pattern and it allowed for several vertical flexural cracks to form giving warnings prior to failure. The number and width of these cracks differ with the PVA%, a/d, and stirrups. PVA-mortar beam specimens showed less but wider cracks prior to failure compared to the beam specimens without PVA fibres.

Reducing a/d led to raising first crack loads and ultimate loads, improving ductility and, in turn, shear capacity without changing the mode of failure. The utmost enhancement in the performance of the test beams was achieved with PVA fibres content of 2.25% and a/d equals 1.5 where the enhancement of energy absorption was 365% over that in a beam without fibres.

PVA played the same role as the stirrups and contributed to the shear behaviour of studied beams. The contribution of PVA to ultimate shear capacity was increased with reducing the amount of shear reinforcement (stirrups).

Table 11 Comparison between experimental and predicted ultimate shear strength results

Group	Beam	$V_{\mathrm{u,\ exp.}}$, kN	$V_{\mathrm{u,\ Anal.}}$, kN	$V_{\mathrm{u,exp.}}/V_{\mathrm{u,Anal}}$
Group A	B1	89.50	78.00	1.14
	B2	134.25	122.00	1.10
	B3	170.00	181.00	0.94
	B4	203.25	229.00	0.89
Group B	B5	95.35	80.00	1.191
	B6	148.00	124.00	1.194
	B7	232.00	195.00	1.190
	B8	264.00	251.00	1.052
Group C	B9	189.00	217.00	0.88
	B10	201.00	228.00	0.89
	B11	234.50	250.00	0.94
Group D	B12	163.30	154.00	1.060
	B13	173.10	177.00	0.97
	B14	200.00	195.00	1.026
Group E	B15	118.00	116.00	1.017
	B16	138.00	140.00	0.98
	B17	170.00	163.00	1.044
Average				1.038
Standard deviation				0.11
Coefficient of variation				10.50%

PVA played a significant role in beam specimens without stirrups. In addition, the PVA fibres were more effective for lower shear span to depth ratio (a/d = 1.5), where the enhancement of shear resistance was 221%.

For the tested PVA beams in the current study, the specimens were numerically modeled using the non-linear finite element NLFEA model using ANSYS software. The PVA fibres were simulated as smeared reinforcements in the mortar elements represented through volumetric ratio to represent the actual fibre volumes used in each beam specimen. The predicted crack pattern and load–deflection curves showed excellent agreement with the experimentally reported ones. The ratio of the predicted to experimental ultimate strength ranged between 0.91 and 1.09.

A proposed equation was developed in the current research which is a modification of CSA Standard [35] design equation. Good agreement was achieved between the experimental and predicted shear strength results. The ratios of [$V_{u,\ exp.}/V_{u,\ Anal.}$] for the studied beams ranged between 0.84 and 1.29.

Based on the results of the current study and for practical applications, the authors recommend a combination of fly ash, silica fume and at least 1.5% PVA in the presence of minimum stirrups reinforcement (5Φ6/m) or adding 2.25% PVA without stirrups to achieve adequate shear behaviour of PVA-mortar beams. This combination prevented sudden failure and improved the ductility as several small flexural cracks were formed prior to failure.

Funding The authors declare that they have no known competing financial interests or personal relationships that could have appeared to influence the work reported in this paper. The authors state that they did not get any funding for this research and it is self-funded.

Declarations

Conflict of interest The authors declare that they have no conflict of interest.

Human and animal rights This article does not contain any studies with human participants or animals performed by any of the authors.

References

1. Pan Z, Wu C, Jianzhong L, Wang W, Jiwei L (2015) Study on mechanical properties of cost-effective polyvinyl alcohol engineered cementitious composites (ECC-PVA). Construct Build Mater 78:397–404
2. Li VC, Wu C, Wang SX, Ogawa A, Saito T (2002) Interface tailoring for strain-hardening polyvinyl alcohol-engineered cementitious composite (PVA-ECC). ACI Mater J 99(5):463–472
3. Li VC (1998) Engineered cementitious composites—tailored composites through micromechanical modeling. In: Banthia N, Bentur A, Mufti AA (eds) Fiber reinforced concrete: present and the future. Canadian Society for Civil Engineering, Montreal, pp 64–97
4. Iqbal Khan M, Fares G, Mourad S (2017) Optimized fresh and hardened properties of strain hardening cementitious composites: effect of mineral admixtures, cementitious composition, size, and type of aggregates. J Mater Civ Eng 29(10):04017178-1–16
5. Li, Victor C (1993) From Micromechanics to structural engineering - the design of cementitous composites for civil engineering applications. JSCE J Struct Mech Earthq Eng JSCE J 10(2): 37–48, http://hdl.handle.net/2027.42/84735.
6. Zhang R, Matsumoto K, Niwa J, Hirata T, Ishizeki Y (2013) Experimental study on shear behaviour of PP-ECC BEAMS with different stirrups Ratios. In: Proceedings of the Thirteenth East Asia-Pacific Conference on structural engineering and construction (EASEC-13), September 11–13, 2013, Sapporo, Japan, B-5–5., B-5–5, http://hdl.handle.net/2115/54260
7. Zhu Y, Zhang Z, Yang Y, Yao Y (2014) Measurement and correlation of ductility and compressive strength for engineered cementitious composites (ECC) produced by binary and ternary systems of binder materials: FLY ash, slag, silica fume and cement. Constr Build Mater 68:192–198
8. Kanda T, Li VC (1998) Interface property and apparent strength of high-strength hydrophilic fibre in cement matrix. J Mater Civ Eng 10(1):5–13
9. Kanda T, Watanabe S (1998) Application of pseudo strain hardening cementitious composites to shear resistant structural elements", fracture mechanics of concrete structures. In: Proceedings FRAMCOS-3, AEDIFICATIO Publishers, D-79104 Freiburg, Germany, 1998, pp. 1477–1490.
10. Alyousif A, Anil O, Sahmaran M, Lachemi M, Yildirim G, Ashour A (2016) Comparison of shear behaviour of engineered cementitious composite and normal concrete beams with different shear span lengths. Mag Concr Res 68(5):217–228. https://doi.org/10.1680/jmacr.14.00336 (**Paper 1400336**)
11. Paegle I, Fischer G (2016) Phenomenological interpretation of the shear behavior of reinforced Engineered Cementitious Composite beams. Cement Concr Compos 73:213–225. https://doi.org/10.1016/j.cemconcomp.2016.07.018
12. Liu H, Zhang Q, Gu C, Su H, Li VC (2017) Self-healing of micro cracks in Engineered Cementitious Composites under sulfate and chloride environment. Constr Build Mater 153(30):948–956. https://doi.org/10.1016/j.conbuildmat.2017.07.126
13. Ismail MK, Hassan AA (2019) Influence of fibre type on the shear behaviour of engineered cementitious composite beams. Mag Concr Res. https://doi.org/10.1680/jmacr.19.00172
14. Liu Y, Zhou X, Lv C, Yang Y, Liu T (2018) Use of silica fume and GGBS to improve frost resistance of ECC with high-volume fly ash, Hindawi. Adv Civ Eng. https://doi.org/10.1155/2018/7987589
15. Wang L, Zhou SH, Shi Y, Tang SW, Chen E (2017) Effect of silica fume and PVA fibre on the abrasion resistance and volume stability of concrete. Compos B 130:28–37
16. EN 197 EN 197–2004 (2004) Cement; Composition, specifications and conformity criteria", European standards (2004/1–197EN)
17. ASTM C 618 (2012) Standard Specification for coal fly ash and raw or calcined natural Pozzolan for use in concrete. ASTM, West Conshohocken, p 3
18. ASTM C1240 (2015) Standard Specification for Silica Fume Used in Cementitious Mixtures, West Conshohocken, Pennsylvania; 2015
19. Cao L (2010) Experimental study on mechanical property of PVA-fiber reinforced cementitious composite. [Master's thesis], Zhengzhou, China: Henan Polytechnic University, 2010
20. Said M, Mustafa TS, Shanour AS, Khalil MM (2020) Experimental and analytical investigation of high performance concrete

beams reinforced with hybrid bars and polyvinyl alcohol fibers. Constr Build Mater 259:1–22. https://doi.org/10.1016/j.conbuildmat.2020.120395
21. Egyptian Standard Specifications (2002) Concrete Aggregates from natural sources", ESS No 1109/2002
22. BS EN 934–2 2009 Edition (2009) Admixtures for concrete, mortar and grout Part 2: Concrete admixtures—definitions, requirements, conformity, marking and labelling
23. Egyptian Standard Specifications, "Steel Reinforcement Bars", No. 262/1999
24. ECP (Egyptian Code of Practice) (2007) ECP 203-2007: design and construction for reinforced concrete structures. Ministry of Building Construction, Research Center for Housing, Building and Physical Planning, Cairo, Egypt
25. Zhou J, Qian S, Ye G, Copuroglu O, Breugel KV, Li VC (2012) Improved fibre distribution and mechanical properties of engineered cementitious composites by adjusting the sequence. Cement Concr Compos 34(3):342–348
26. Meng D, Lee CK, Zhang YX (2017) Flexural and shear behaviours of plain and reinforced polyvinyl alcohol-engineered cementitious composite beams. Eng Struct 151:261–272. https://doi.org/10.1016/j.engstruct.2017.08.036
27. Qudah S, Maalej M (2014) Applications of engineered cementitious composites (ECC) in interior beam-column connections for enhance seismic resistance. Eng Struct 69:235–245. https://doi.org/10.1016/j.engstruct.2014.03.026
28. Hasib M, Hossain K (2016) Shear resistance of composite beams without shear reinforcement. In: Resilient Infrastructure Conference, June 1–4, 2016, pp. STR-928–1–8
29. Shimizu K, Kanakubo T, Kanda T, Nagai S (204) Shear behavior of steel reinforced ECC-PVA beams. In: 13th World Conference on Earthquake Engineering, Vancouver, B.C., Canada, August 1–6, 2004, Paper No. 704
30. Said M, Abd-Elazim A, Ali M, Elghazaly H, Shaaban IG (2020) Effect of elevated temperature on axially and eccentrically loaded columns containing polyvinyl alcohol (PVA) fibres. Eng Struct. https://doi.org/10.1016/j.engstruct.2019.110065
31. Hossain KMA, Hasib S, Manzur T (2020) Shear behavior of novel hybrid composite beams made of self-consolidating concrete and engineered cementitious composites. Eng Struct 202:109856
32. ANSYS–Release Version 14.5 (2012) A finite element computer software and user manual for nonlinear structural analysis. ANSYS Inc., CanonsburgA
33. Shanour AS, Said M, Arafa AA, Adam A (2018) Flexural performance of concrete beams containing engineered cementitious composites. Constr Build Mater 180:23–34
34. Soroushian P, Lee C-D (1989) Constitutive modeling of steel fiber reinforced concrete under direct tension and compression. Fiber reinforced cements and concrete: recent developments. In: Proceedings of an International Conference held at the University of Wales, College of Cardiff, School of Engineering, UK, Sep. 18-20, 1989, pp 363–377
35. CSA Standard A23.3–04 (2004) Canadian standard association (CSA). Design of concrete structures, CSA standard A23.3–04, Rexdale, Ontario. 2004.
36. Beshara FB, Mustafa TS, Mahmoud AA, Khalil M (2020) Constitutive models for nonlinear analysis of SFRC Corbels. J Build Eng 28:1–15. https://doi.org/10.1016/j.jobe.2019.101092
37. Yang E, Li VC (2010) Strain-hardening fiber cement optimization and component tailoring by means of a micromechanical model. Constr Build Mater 24:130–139